Plattenbauten: Touching Rectangles in Space*

Stefan Felsner†
Institut für Mathematik
Technische Universität Berlin

Kolja Knauer
Departament de Matemàtiques i Informàtica,
Universitat de Barcelona
and
Aix-Marseille Univ, Université de Toulon,
CNRS, LIS, Marseille

Torsten Ueckerdt
Institute for Theoretical Informatics,
Karlsruhe Institute of Technology (KIT)

Planar bipartite graphs can be represented as touching graphs of horizontal and vertical segments in $\mathbb{R}^2$. We study a generalization in space: touching graphs of axis-aligned rectangles in $\mathbb{R}^3$, and prove that planar 3-colorable graphs can be represented this way. The result implies a characterization of corner polytopes previously obtained by Eppstein and Mumford. A by-product of our proof is a distributive lattice structure on the set of orthogonal surfaces with given skeleton.

Further, we study representations by axis-aligned non-coplanar rectangles in $\mathbb{R}^3$ such that all regions are boxes. We show that the resulting graphs correspond to octahedrations of an octahedron. This generalizes the correspondence between planar quadrangulations and families of horizontal and vertical segments in $\mathbb{R}^2$ with the property that all regions are rectangles.

Keywords: Touching graphs, contact graphs, boxicity, planar graphs

1 Introduction

The importance of contact and intersection representations of graphs stems not only from their numerous applications including information visualization, chip design, bio informatics and robot motion planning (see for example the references in [2, 11]), but also from the structural and algorithmic insights accompanying the investigation of these intriguing geometric arrangements. From a structural point of view, the certainly most fruitful contact representations (besides the "Kissing Coins" of Koebe, Andrew, and Thurston [1,22,29]) are axis-aligned segment contact representations: families of interior-disjoint horizontal and vertical segments

*An extended abstract appears in the proceedings of the 46th International Workshop on Graph-Theoretic Concepts in Computer Science (WG 2020) [14].
†Partially supported by DFG grant FE-340/11-1.

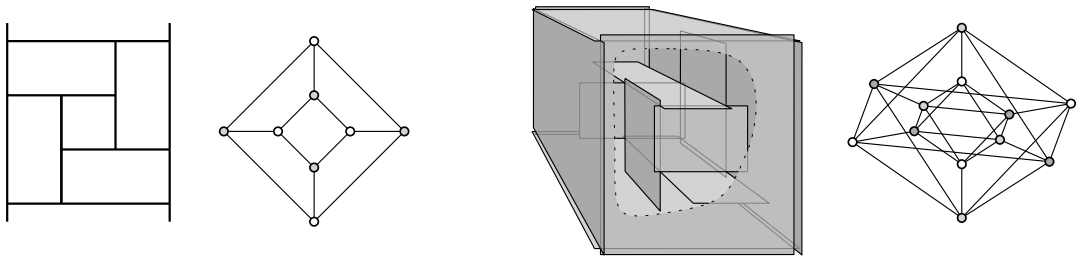

Figure 1: An axis-aligned segment contact representation (left) and a Plattenbau (right) together with the respective touching graphs.

in $\mathbb{R}^2$ where the intersection of any two segments is either empty or an endpoint of at least one of the segments. The corresponding touching graph[1] has the segments as its vertices and the pairs of segments as its edges for which an endpoint of one segment is an interior point of the other segment, see the left of Figure 1. It has been discovered several times [20, 27] that any such touching graph is bipartite and planar, and that these two obviously necessary conditions are in fact already sufficient: Every planar bipartite graph is the touching graph of interior-disjoint axis-aligned segments in $\mathbb{R}^2$. In fact, edge-maximal segment contact representations endow their associated plane graphs with many useful combinatorial structures such as 2-orientations [11], separating decompositions [4], bipolar orientations [28, 30], transversal structures [16], and Schnyder woods [32].

In this paper we extend axis-aligned segment contact representations in $\mathbb{R}^2$ to axis-aligned rectangle contact representations in $\mathbb{R}^3$. That is, we consider families $\mathcal{R}$ of axis-aligned closed and bounded rectangles in $\mathbb{R}^3$ with the property that for all $R, R' \in \mathcal{R}$ the intersection $R \cap R'$ is a subset of the boundary of at least one of them, i.e., the rectangles are interiorly disjoint. We call such a family a *Plattenbau*[2]. Given a Plattenbau $\mathcal{R}$ one can consider its *intersection graph* $I_{\mathcal{R}}$, see Section 5. However, for us the more important concept is a certain subgraph of $I_{\mathcal{R}}$, called the *touching graph* $G_{\mathcal{R}}$ of $\mathcal{R}$. There is one vertex in $G_{\mathcal{R}}$ for each rectangle in $\mathcal{R}$ and two vertices are adjacent if the corresponding rectangles *touch*, i.e., their intersection is non-empty and contains interior points of one and only one of the rectangles. We say that G is a *Plattenbau graph* if there is a Plattenbau $\mathcal{R}$ such that $G \cong G_{\mathcal{R}}$. In this case we call $\mathcal{R}$ a *Plattenbau representation* of G.

Plattenbau

touching graph

touch

Plattenbau graph

Plattenbau representation

Plattenbauten are a natural generalization of axis-aligned segment contact representations in $\mathbb{R}^2$ and thus Plattenbau graphs are a natural generalization of planar bipartite graphs. While clearly all Plattenbau graphs are tripartite (properly vertex 3-colorable), it is an interesting challenge to determine the exact topological properties in $\mathbb{R}^3$ that hold for all Plattenbau graphs, thus generalizing the concept of planarity from 2 to 3 dimensions (for tripartite graphs). We present results towards a characterization of Plattenbau graphs in three directions.

Our Results and Organization of the Paper. In Section 2 we provide examples of Plattenbau graphs and give some necessary conditions for all Plattenbau graphs. We observe that unlike touching graphs of segments, general Plattenbau graphs are not closed under taking subgraphs.

[1] We use the term touching graphs rather than the more standard contact graph to underline the fact that segments with coinciding endpoints (e.g., two horizontal segments touching a vertical segment in the same point but from different sides, but also non-parallel segments with coinciding endpoint) do not form an edge.

[2] Plattenbau (plural Plattenbauten) is a German word describing a building (*Bau*) made of prefabricated concrete panels (*Platte*).

We circumvent this issue by restricting ourselves to generic Plattenbauten, i.e., $\mathcal{R}$ contains no coplanar rectangles. Moreover, we introduce boxed Plattenbauten where every bounded region of $\mathbb{R}^3$ is a box, and discuss questions of augmentability.

In Section 3 we show that within planar graphs the necessary condition of 3-colorability is also sufficient for Plattenbau graphs. Thus, the topological characterization of Plattenbau graphs must fully contain planarity (which is not obvious as we consider 3-colorable graphs and not only bipartite graphs).

Theorem 1. *Every 3-colorable planar graph is the touching graph of a generic Plattenbau.*

A critical part of proof of Theorem 1 is a characterization of skeletons of orthogonal surfaces as the duals of babet-free eulerian triangulations in Section 3.1 and Proposition 4. This characterization is equivalent to a characterization of the graphs of corner polyhedra previously given by Eppstein and Mumford [7, Theorem 3]. Another proof of Theorem 1 can be obtained from Gonçalves' proof that 3-colorable planar graphs admit segment intersection representations with segments of 3 slopes [18]. We further comment on these alternative approaches in Section 3.3. A consequence of our approach is a natural partial order - namely a distributive lattice - on the set of orthogonal surfaces with a given skeleton.

In Section 4 we consider generic and boxed Plattenbau graphs as the 3-dimensional analogue of edge-maximal planar bipartite graphs, the quadrangulations. We give a complete characterization:

Theorem 2. *A graph* G *is the touching graph of a generic boxed Plattenbau* $\mathcal{R}$ *if and only if there are six outer vertices in* G *such that each of the following holds:*

(P1) G *is connected and the outer vertices of* G *induce an octahedron.*

(P2) The edges of G *admit an orientation such that*

- *the bidirected edges are exactly the outer edges,*
- *each vertex has exactly 4 outgoing edges.*

(P3) The neighborhood $N(v)$ *of each vertex* v *induces a spherical quadrangulation* $SQ(v)$ *in which the out-neighbors of* v *induce a 4-cycle.*

- *If* v *is an outer vertex, this 4-cycle bounds a face of* $SQ(v)$.

(P4) For every edge uv *of* G *with common neighborhood* $C = N(u) \cap N(v)$*, the cyclic ordering of* C *around* u *in* $SQ(v)$ *is the reverse of the cyclic ordering of* C *around* v *in* $SQ(u)$.

spherical quadrangulation

A *spherical quadrangulation* is a graph embedded on the 2-dimensional sphere without crossings such that each face is bounded by a 4-cycle. Spherical quadrangulations are 2-connected, planar, and bipartite. We remark that Theorem 2 does not give a complete characterization of generic Plattenbau graphs since some generic Plattenbau graphs are not contained in any generic boxed Plattenbau graph as discussed in Section 2.

Let us further remark that we show in Subsection 4.1 how every generic boxed Plattenbau can be constructed in a natural way from trivial parts.

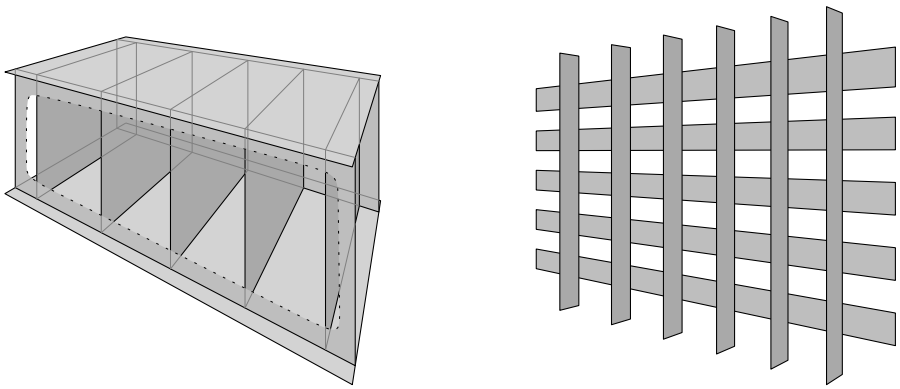

Figure 2: Plattenbau representations of $K_{2,2,5}$ (left) and $K_{5,6}$ (right).

2 Types of Plattenbauten and Questions of Augmentation

Let us observe some properties of Plattenbau graphs. Clearly, the class of all Plattenbau graphs is closed under taking induced subgraphs. Examples of Plattenbau graphs are $K_{2,2,n}$, see Figure 2, and the class of grid intersection graphs, i.e., bipartite intersection graphs of axis-aligned segments in the plane [20]. For the latter take the segment intersection representation of a graph, embed it into the xy-plane in $\mathbb{R}^3$ and thicken all horizontal segments a small amount into y-direction and all vertical segments a bit into z-direction outwards the xy-plane. In particular, $K_{m,n}$ is a Plattenbau graph, see Figure 2. In order to exclude some graphs, we observe some necessary properties of all Plattenbau graphs.

Observation 1. *If* G *is a Plattenbau graph, then*

1. *the chromatic number of* G *is at most 3,*
2. *the neighborhood of any vertex of* G *is planar,*
3. *the* boxicity *of* G*, i.e., the smallest dimension* d *such that* G *is the intersection graph of some boxes in* $\mathbb{R}^d$*, is at most 3.*

Proof. Item 1: Each orientation class is an independent set.

Item 2: Let v be a vertex of G represented by $R \in \mathcal{R}$. Let H be the supporting hyperplane of R and H^+, H^- the corresponding open halfspaces. The neighborhood $N(v)$ consists of rectangles R^+ intersecting H^+ and those R^- intersecting H^-. The rectangles in each of these sets have a plane touching graph, since it corresponds to the touching graph of the axis-aligned segments given by their intersections with R. The neighboring rectangles in $R^+ \cap R^-$ are on the outer face in both graphs in opposite order, so identifying them gives a planar drawing of the graph induced by $N(v)$. See Figure 3 for an illustration.

Item 3: A Plattenbau $\mathcal{R}$ can be transformed into a set $\mathcal{B}$ of boxes such that the touching graph of $\mathcal{R}$ is the intersection graph of $\mathcal{B}$ as follows: First, shrink each rectangle orthogonal to the i-axis by a small enough $\varepsilon > 0$ in both dimensions different from i. As a result, we obtain a set of pairwise disjoint rectangles. Then, expand each such rectangle by ε in dimension i. The obtained set $\mathcal{B}$ of boxes are again interiorly disjoint and all intersections are touchings. □

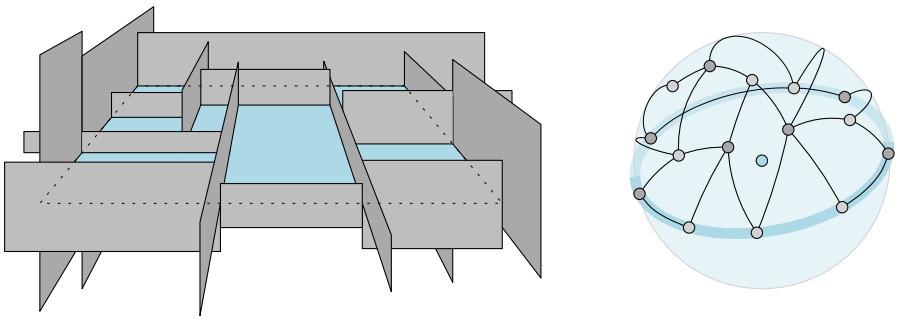

Figure 3: Left: A z-rectangle (depicted in blue) in a Plattenbau with its touching rectangles intersecting its upper halfspace H^+. Right: The resulting crossing-free embedding on the upper hemisphere.

Note that for Items 1 and 2 of Observation 1 it is crucial that G is the touching graph and not the intersection graph. Moreover, Observation 1 allows to reject some graphs as Plattenbau graphs:

- K_4 is not a Plattenbau graph (by Item 1 of Observation 1),
- $K_{1,3,3}$ is not a Plattenbau graph (by Item 2 of Observation 1).
- The full subdivision of $K_{2^{2^5}+1}$ is not a Plattenbau graph (by Item 3 of Observation 1 and [3]).

Remark 1. *The number of vertices of the last example is a 10 digits number. This can be reduced: A class $\mathcal{S}$ of geometric objects in $\mathbb{R}^d$ is t-separable if there exists a family $\mathcal{H} = \{H_1, \ldots, H_t\}$ of hyperplanes, such that any two disjoint elements of $\mathcal{S}$ can be separated by a translate of one of the hyperplanes from $\mathcal{H}$. A family $\mathcal{B}$ of axis-aligned boxes in $\mathbb{R}^3$ is clearly 3-separable. In [12, Prop. 2.3] it has been shown that if G is a bipartite graph admitting a t-separable intersection representation, then the bipartite poset corresponding to G has order dimension at most $2t$. Since it is known that the order dimension of the full subdivision of K_{2647} is 7 (Hoşten and Morris [21]) we conclude:*

- *the full subdivision of K_{2647} is not a Plattenbau graph.*

In particular, some bipartite graphs are not Plattenbau graphs. Together with $K_{m,n}$ being a Plattenbau graph, this shows that the class of Plattenbau graphs is not closed under taking subgraphs; an unusual situation for touching graphs, which prevents us from solely focusing on edge-maximal Plattenbau graphs. To overcome this issue, we say that a Plattenbau $\mathcal{R}$ is *generic* if it contains no co-planar rectangles[3]. In a generic Plattenbau each edge of each rectangle intersects the interior of at most one other rectangle. Thus, if $\mathcal{R}$ is generic, then each edge of the touching graph $G_{\mathcal{R}}$ can be removed by shortening one of the participating rectangles slightly. That is, the class of graphs with generic Plattenbau representations is closed under subgraphs. *generic*

We furthermore say that a Plattenbau $\mathcal{R}$ is *boxed* if six *outer rectangles* constitute the *boxed*

[3] In the conference version of this paper, we worked with a more restrictive version of "proper" Plattenbau, where for any two touching rectangles R, R' the intersection $R \cap R'$ must be a boundary edge of one of R and R'. However, there was a mistake in one proof whence we cannot ensure such a representations for planar 3-chromatic graphs.

sides of a box that contains all other rectangles and all regions inside this box are also boxes. (A box is an axis-aligned full-dimensional cuboid, i.e., the Cartesian product of three bounded intervals of non-zero length. And a region is a connected component of $\mathbb{R}^3$ after the removal of all rectangles in $\mathcal{R}$.) For boxed Plattenbauten we use the additional convention that the edge-to-edge intersections of outer rectangles yield edges in the touching graph, even though these intersections contain no interior points[4]. In particular, the outer rectangles of a generic boxed Plattenbau induce an octahedron in the touching graph.

Observation 2. *The touching graph $G_{\mathcal{R}}$ of a generic Plattenbau $\mathcal{R}$ with $n \geq 6$ vertices has at most $4n-12$ edges. Equality holds if $\mathcal{R}$ is boxed.*

Proof. As noted above, for a generic Plattenbau $\mathcal{R}$ with touching graph $G_{\mathcal{R}}$ there is an injection from the edges of $G_{\mathcal{R}}$ to the edges of rectangles in $\mathcal{R}$: For each edge uv in $G_{\mathcal{R}}$ with corresponding rectangles $R_u, R_v \in \mathcal{R}$, take the edge of R_u or R_v that contributes to their intersection $R_u \cap R_v$. This way, each of the four edges of each of the n rectangles in $\mathcal{R}$ corresponds to at most one edge in $G_{\mathcal{R}}$.

If in for one of the three orientations, $\mathcal{R}$ contains at most one rectangle in that orientation, then $G_{\mathcal{R}}$ is a planar bipartite graph plus one additional vertex. In particular, $G_{\mathcal{R}}$ has at most $2(n-1)-4+(n-1) < 4n-12$ edges, as long as $n \geq 6$.

Now let $\mathcal{R}$ contain at least two rectangles of each orientation. The two extreme rectangles of each orientation are the 6 *special* rectangles. The hyperplanes supporting the special rectangles form a box B. We plan to attribute to each special rectangle a loss of two out of the $4n$ potential edges of $G_{\mathcal{R}}$. Let S be a special rectangle and s be an edge of $S \cap B$. If s is not touching another rectangle, then s contributes to the loss. If s is touching a non-special rectangle R, then R extends beyond B and has a boundary edge which is not touching another rectangle, this loss can be attributed to s. Finally, if s is touching a special rectangle, then the corresponding edge of $G_{\mathcal{R}}$ can be assigned to s and to an edge of the other special rectangle. In this case we charge a loss of $1/2$ to s. Hence, each of the 24 edges of the 6 special rectangles contributes a loss of at least $1/2$ and $G_{\mathcal{R}}$ has at most $4n-12$ edges.

If $\mathcal{R}$ is boxed, then the above analysis is tight, i.e., $G_{\mathcal{R}}$ has exactly $4n-12$ edges. □

An immediate consequence of Observation 2 is that $K_{5,6}$ is a Plattenbau graph which has no generic Plattenbau representation. Contrary to the case of axis-aligned segments in $\mathbb{R}^2$, neither can every generic Plattenbau in $\mathbb{R}^3$ be completed to a boxed Plattenbau, nor is every boxed Plattenbau equivalent to a generic one. See Figure 4 for problematic examples. The example on the left is generic, but it is not a subgraph of a Plattenbau graph with a generic and boxed Plattenbau representation. The touching graph of the example on the right is 7-regular and has 12 vertices, i.e., 42 edges. Hence, by Observation 2 it has too many edges to be the touching graph of a generic Plattenbau.

3 Planar 3-Colorable Graphs

Let us recall the main result of this section:

Theorem 1. *Every 3-colorable planar graph is the touching graph of a generic Plattenbau.*

[4] The edges between the outer rectangles could also be realized with standard touchings: just extend the six rectangles of the enclosing box appropriately. The six outer rectangles of Figure 1 form such an extended box.

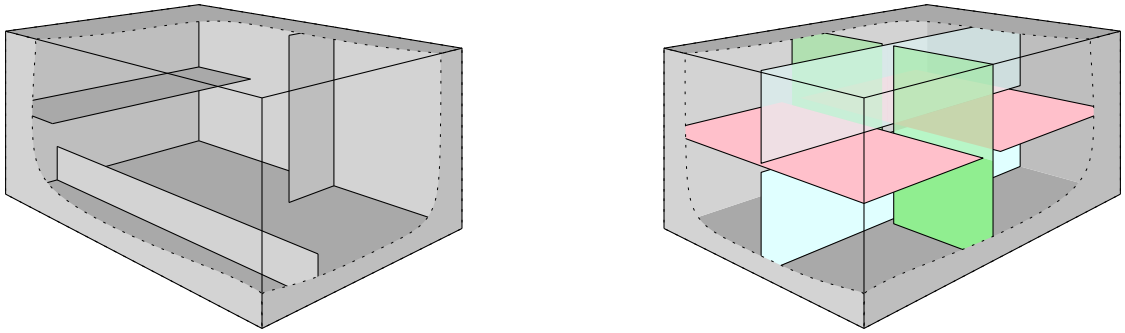

Figure 4: A generic Plattenbau that cannot be augmented to a boxed Plattenbau and a boxed Plattenbau that is not generic.

The proof of this theorem is in several steps. First we introduce orthogonal surfaces and show that the dual graph of the skeleton of an orthogonal surface is a Plattenbau graph (Proposition 3). In the second step we characterize triangulations whose dual is the skeleton of an orthogonal surface (Section 3.1 and Proposition 4). One consequence of this is a natural very well-behaved partial order, namely a distributive lattice, on the set of orthogonal surfaces with given skeleton (Corollary 5). We then show that a Plattenbau representation of a 3-colorable triangulation can be obtained by patching orthogonal surfaces in corners of orthogonal surfaces (Section 3.2).

We begin with an easy observation.

Observation 3. *Every 3-colorable planar graph* G *is an induced subgraph of a 3-colorable planar triangulation.*

Sketch. Consider G with a plane embedding. By adding just subdivided edges we find a 2-connected 3-colorable G' which has G as an induced subgraph.

Fix a 3-coloring of G'. Let f be a face of G' of size at least four and c be a color such that at least three vertices of f are not colored c. Stack a vertex v inside f and connect it to the vertices on f that are not colored c. The new vertex v is colored c and the sizes of the new faces within f are 3 or 4. After stacking in a 4-face, the face is either triangulated or there is a color which is not used on any newly created 4-face. An additional stacking triangulates the 4-face. □

A plane triangulation T is 3-colorable if and only if it is Eulerian. Hence, the dual graph T^* of T apart from being 3-connected, cubic, and planar is also bipartite. The idea of the proof is to find an orthogonal surface $\mathfrak{S}$ such that T^* is the skeleton of $\mathfrak{S}$. This is not always possible but with a technique of patching one orthogonal surface in an appropriate corner of a Plattenbau representation obtained from another orthogonal surface, we shall get to a proof of the theorem.

Consider $\mathbb{R}^3$ with the *dominance order*, i.e., $x \leq y$ if and only if $x_i \leq y_i$ for $i = 1, 2, 3$. The join and meet of this distributive lattice are the componentwise max and min. Let $\mathcal{V} \subseteq \mathbb{R}^3$ be a finite *antichain*, i.e., a set of mutually incomparable points. The *filter* of $\mathcal{V}$ is the set $\mathcal{V}^\uparrow := \{x \in \mathbb{R}^3 \mid \exists v \in \mathcal{V} : v \leq x\}$ and the boundary $\mathfrak{S}_\mathcal{V}$ of $\mathcal{V}^\uparrow$ is the *orthogonal surface* generated by $\mathcal{V}$. The left part of Figure 5 shows an example in $\mathbb{R}^3$. The nine vertices of the *generating set* $\mathcal{V}$ are emphasized.

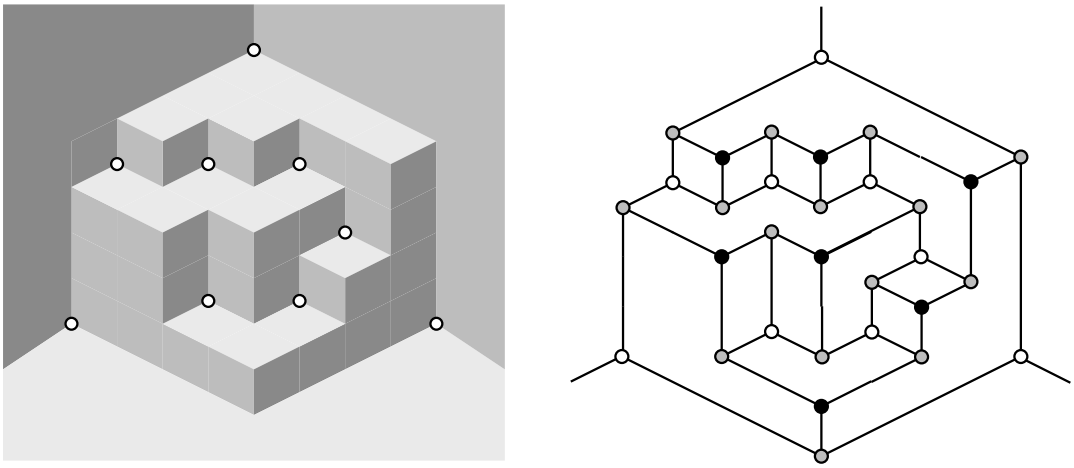

Figure 5: An orthogonal surface and its skeleton (vertex v_∞ omitted).

Orthogonal surfaces have been studied by Scarf [19] in the context of test sets for integer programs. They later became of interest in commutative algebra, cf. the monograph of Miller and Sturmfels [26]. Miller [25] observed the connections between orthogonal surfaces, Schnyder woods and the Brightwell-Trotter Theorem about the order dimension of polytopes, see also [9].

A maximal connected set of points of an orthogonal surface which is constant in one of the coordinates is called a *flat*. A non-empty intersection of two flats is an *edge*. A point contained in three flats is called a *vertex*. An edge incident to only one vertex is a *ray*.

An orthogonal surface is *tame* if the following two non-degeneracy conditions hold:

(1) Every vertex has degree exactly three. (2) There are exactly three rays.

In this paper we use the term *orthogonal surface* as a synonym for tame orthogonal surface.

orthogonal surface

The *skeleton* $G_{\mathcal{S}}$ of an orthogonal surface $\mathcal{S}$ is the graph consisting of the vertices and edges of the surface, in addition there is a vertex v_∞ which serves as second vertex of each ray. The skeleton graph is planar, cubic, and bipartite. The bipartition consists of the maxima and minima of the surface in one class and of the saddle vertices in the other class. The vertex v_∞ is a saddle vertex. The dual of $G_{\mathcal{S}}$ is a triangulation with a designated outer face, the dual of v_∞.

skeleton

The generic structure of a bounded flat is as shown in Figure 6; the boundary consists of two zig-zag paths sharing the two *extreme points* of the flat. The minima of the *lower* zig-zag are elements of the generating set $\mathcal{V}$, they are minimal elements of the orthogonal surface $\mathcal{S}$. The maxima of the *upper* zig-zag are maximal elements of $\mathcal{S}$. The maxima can be considered to be *dual generators* of $\mathcal{S}$.

With the following proposition we establish a first connection between orthogonal surfaces and Plattenbau graphs.

Proposition 3. *The dual triangulation of the skeleton of an orthogonal surface $\mathcal{S}$ obeying the two non-degeneracy conditions is a Plattenbau graph and admits a generic Plattenbau representation.*

Proof. Choose an interior point in each of the three rays of $\mathcal{S}$ and call these points the extreme points of their incident unbounded flats.

The two extreme points a_f, b_f of a flat f of $\mathcal{S}$ span a rectangle $R(f)$. Note that the other two corners of $R(f)$ are $\max(a_f, b_f)$ and $\min(a_f, b_f)$. We claim that the collection of rectangles $R(f)$

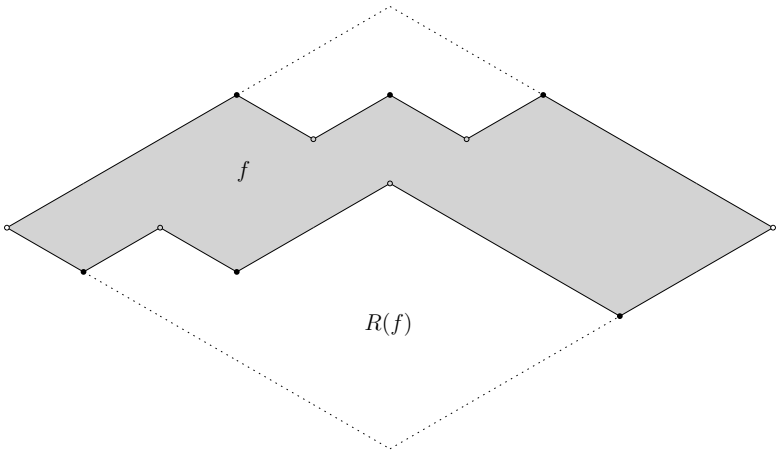

Figure 6: Generic flat f and the spanned rectangle $R(f)$.

weak representation

is a *weak* rectangle contact representation of the dual triangulation T of the skeleton of $\mathfrak{S}$. Here weak means that the contacts of pairs of rectangles of different orientation can be an edge to edge contact.

Let f and f' share an edge e of the skeleton, we have to show that $R(f)$ and $R(f')$ are in contact. One of the ends of e is a saddle point of $\mathfrak{S}$ and thus extreme in two of its incident flats. Hence, it is extreme for at least one of f and f'. This shows that e is contained in the boundary of at least one of the rectangles $R(f), R(f')$, i.e., the intersection of the open interiors of the rectangles is empty and the intersection of $R(f)$ and $R(f')$ is a contact.

We now show that besides contacts induced by edges of the skeletons there are no intersections of recangles $R(f)$ and $R(f')$. Consider two flats f and f' and let H_f and $H_{f'}$ be the supporting planes. If f is contained in an open halfspace O defined by $H_{f'}$, then $\max(a_f, b_f)$ and $\min(a_f, b_f)$, the other two corners of $R(f)$, are also in O, hence $R(f)$ is completely contained in O and $R(f) \cap R(f') = \emptyset$. If f intersects $H_{f'}$ and f' intersects H_f, then consider the line $\ell = H_{f'} \cap H_f$. This line is parallel to one of the axes, hence it intersects $\mathfrak{S}$ in a closed interval $I_{\mathfrak{S}}$. If I_f and $I_{f'}$ are the intervals obtained by intersecting ℓ with f and f' respectively, then one of them equals $I_{\mathfrak{S}}$ and the other is an edge of the skeleton of $\mathfrak{S}$, i.e., (f, f') is an edge of the triangulation T.

It remains to expand some of the rectangles to change weak contacts into true contacts. Let $e = f \cap f'$ be an edge such that the contact of $R(f)$ and $R(f')$ is weak. Select one of f and f', say f. Now expand the rectangle $R(f)$ with a small parallel shift of the boundary segment containing e. This makes the contact of $R(f)$ and $R(f')$ a true contact. The expansion can be taken small enough as to avoid that new contacts or intersections are introduced. Iterating over the edges we eventually get rid of all weak contacts. See Figure 7 for an illustration.

In an orthogonal surface some flats might be co-planar. But by non-degeneracy all vertices are of degree three. Thus, flats (and the corresponding rectangles) can be perturbed slightly into the orthogonal direction such that co-planarity is avoided. This concludes the construction. □

Recall that we aim at realizing T^*, the dual of the 3-colorable triangulation T as the skeleton of an orthogonal surface. Since T is Eulerian its dual T^* is bipartite. Let U (black) and U' (white) be the bipartition of the vertices of T^* such that the dual v_∞ of the outer face of T

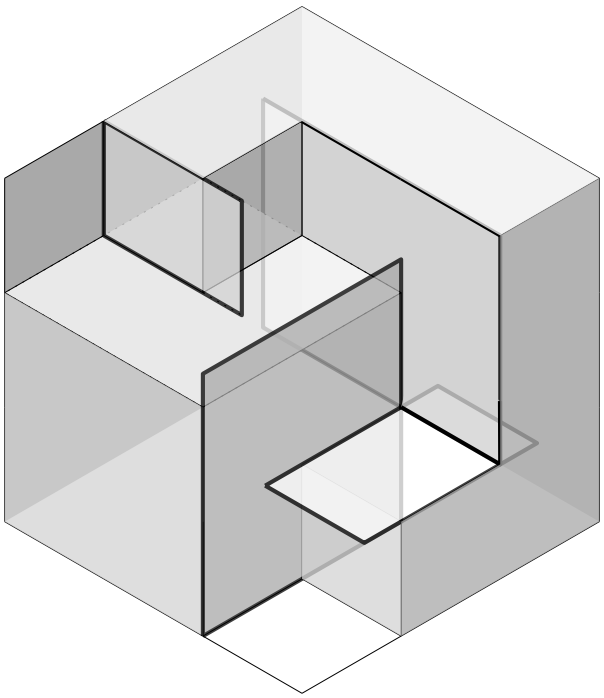

Figure 7: Replacing flats by rectangles and expanding in order to avoid weak contacts.

is in U. The critical task is to assign two extreme vertices to each face of T^* such that v_∞ is never assigned. This has to be done so that each vertex in U (except v_∞) is extremal for exactly two of the faces.

To solve the assignment problem we will work with an auxiliary graph H_T. The faces of T^* which do not contain v_∞ correspond to the interior vertices of T, we denote this set with V°. As the vertices of T^* are the facial triangles of T, we think of U as representing the black triangles of T. We also let $U^\circ = U - v_\infty$, this is the set of bounded black triangles of T. The vertices of H_T are $V^\circ \cup U^\circ$ the edges of H_T correspond to the incidence relation in T^* and T respectively, i.e., v, u with $v \in V^\circ$ and $u \in U^\circ$ is an edge if vertex v is a corner of the black triangle u. A valid assignment of extreme vertices is equivalent to an orientation of H_T such that each vertex $v \in V^\circ$ has outdegree two and each vertex $u \in U^\circ$ has indegree two, i.e., the outdegrees of the vertices are prescribed by the function α with $\alpha(v) = 2$ for $v \in V^\circ$ and $\alpha(u) = \deg(u) - 2$ for $u \in U^\circ$. Since $|V^\circ| = |U^\circ| = n - 3$ it is readily seen that the sum of the α-values of all vertices equals the number of edges of H_T.

Orientations of graphs with prescribed out-degrees have been studied, e.g., in [10], there it is shown that the following necessary condition is also sufficient for the existence of an α-orientation. For all $W \subset V^\circ$ and $S \subset U^\circ$ and $X = W \cup S$

$$\sum_{x \in X} \alpha(x) \leq |E[X]| + |E[X, \overline{X}]|. \qquad (\alpha)$$

Here $E[X]$ and $E[X, \overline{X}]$ denote the set of edges induced by X, and the set of edges in the cut defined by X, respectively.

Inequality (α) does not hold for all triangulations T and all X. We next identify specific sets X violating the inequality, they are associated to certain **ba**dly **be**having **t**riangles, which we

will call babets for short. In Proposition 4 we then show that babets are the only obstructions for the validity of (α).

Let Δ be a separating triangle of T such that the faces of T bounding Δ from the outside are white. Let W be the set of vertices inside Δ and let S be the collection of black triangles of T which have all vertices in W. We claim that $X = W \cup S$ is violating (α). If $|W| = k$ and $|S| = s$, then $\sum_{x \in X} \alpha(x) = 2|W| + |S| = 2k + s$. The triangulation whose outer boundary is Δ has $2(k+3) - 4$ triangles, half of them, i.e., $k+1$, are black and interior. The right side of (α) is counting the number of incidences between vertices of W and black triangles. Black triangles in Δ have $3(k+1)$ incidences in total. There are $k+1-s$ black triangles which have an incidence with a corner of Δ and 3 of them have incidences with two corners of Δ. Hence the value on the right side is $3(k+1) - (k+1-s) - 3 = 2k + s - 1$. This shows that the inequality is violated. A separating triangle Δ of T with white touching triangles on the outside is called *babet*. *babet*

Proposition 4. *If T has no babet, then there is an orientation of H_T whose outdegrees are as prescribed by α.*

Before we prove Proposition 4 and Theorem 1, let us briefly summarize the procedure.

First, we construct a Plattenbau representation in the babet-free case (Section 3.1) based on an auxiliary graph G arising from the bipartition of T^*, and a Schnyder wood S for G. We then find an orthogonal surface $\mathfrak{S}$ based on the Schnyder wood S and show that the skeleton $G_{\mathfrak{S}}$ of $\mathfrak{S}$ is T^*, which together with Proposition 3 gives a Plattenbau for T. This yields a characterization of skeletons of orthogonal surfaces as the duals of babet-free eulerian triangulations. An equivalent characterization was previously obtained by Eppstein and Mumford [7, Theorem 3] in the terminology of corner polyhedra. In Section 3.3 we comment of the differences in the proofs.

In Section 3.2 we deal with triangulations T which contain babets. The idea is to cut the triangulation T along an innermost babet, find orthogonal surfaces for the orthogonal surfaces for the inside and outside, and patch the former into a saddle point of the latter.

Now, let us start with the proof of Proposition 4.

Proof. Suppose that there is an $X = W \cup S$ violating inequality (α). We are going to modify X in several steps always maintaining the property that the inequality is violated. At the end we will be able to point to a babet in T.

Suppose there is a $u \in S$ with $a \leq 2$ neighbors in W. Let $X' = X - u$ when going from X to X' the left side of (α) is loosing $\deg(u) - 2$ while on the right side we loose the $\deg(u) - a$ edges of H_T which are incident to u but not to W. Since $a \leq 2$ the set X' is violating. From now on we assume that every $u \in S$ has 3 neighbors in W, in particular $\alpha(u) = 1$.

Now the left side of (α) equals $2|W| + |S|$ and for the right side we have $|E[X]| = 3|S|$ and $E[X, \overline{X}]$ contains no edge incident to S. We define $\partial W = |E[X, \overline{X}]|$ the notation indicates that we only have to care of boundary edges of W. The assumption that Inequality (α) is violated then becomes $2|W| + |S| > 3|S| + \partial W$ or equivalently

$$2|W| > 2|S| + \partial W. \qquad (\partial)$$

We can assume that the subgraph of H_T induced by X is connected, otherwise a connected component would also violate the inequality. Let $|W| = k$ and $|S| = s$. The set S is a set of black triangles in the triangulation T and W is the set of vertices of these triangles. Let T_S be

the plane embedding of all edges of triangles of S as seen in T. Classify the faces of T_S as black triangles, white triangles and big faces, and let their numbers be s, t and g, respectively. We consider the outer face of T_S a big face independent of its size, therefore, $g \geq 1$. Consider the triangulation T_S^+ obtained by stacking a new vertex in each big face and connecting it to all the angles of the face, i.e., the degree of the vertex z_f stacked into face f equals the length r_f of the boundary of f. Note that T_S^+ may have multi-edges but every face of T_S^+ is a triangle so that Euler's formula holds. Let $R = \sum_f r_f$ be the sum of degrees of the stack vertices. Since T_S^+ has $k+g$ vertices it has $2(k+g)-4$ faces. However, we also know that T_S^+ has $s+t+R$ faces. Counting the edges incident to the triangles of S we obtain $3s = 3t + R$. Using this to eliminate t we obtain $2(k+g)-4 = 2s + \frac{2R}{3}$, i.e., $2|W| = 2|S| + 4 - 2g + \frac{2R}{3}$. With (∂) this implies $4 + \frac{2R}{3} > \partial W + 2g$.

Claim 1. R *is divisible by 3.*

Proof of Claim. Actually we prove that each r_f is divisible by 3. Let Y be a collection of triangles in a 3-colorable triangulation and let γ be the boundary of Y, i.e., γ is the set of edges incident to exactly one triangle from Y. Let Y_b and Y_w be the black and white triangles in Y and let γ_b and γ_w be the edges of γ which are incident to black and white triangles of Y. Double counting the number of edges in Y we get $3|Y_b| + |\gamma_w| = 3|Y_w| + |\gamma_s|$, hence, $|\gamma_w| \equiv |\gamma_s| \mod 3$. In our case $|\gamma_s| = 0$ and depending on the chosen Y either $R = |\gamma_w|$ or $r_f = |\gamma_w|$. △

Let γ be the boundary cycle of a big face of T_S which is not the outer face. We have seen that $|\gamma| \equiv 0 \mod 3$. We are interested in the contribution of γ to ∂W, i.e., in the number of incidences of vertices of γ with black triangles in the inside of the big face. For convenience we can use multiple copies of a vertex to make γ simple. We let T_γ be the triangulation of the hole. The claim below implies that $\partial\gamma \geq 2|\gamma|/3$, unless $|\gamma| \leq 6$ and there is at most one black triangle in T_γ. Add all the inner black triangles of γ to S and all the inner vertices to W and consider the effect for the violator inequality $4 + \frac{2R}{3} > \partial W + 2g$. In the exceptional case we only have one black triangle and $|\gamma| = 6$, i.e., the left side is reduced by 4 and the right side by $3+2$. In all other cases the left side of the violator inequality is reduced by $2|\gamma|/3$ and the right side is reduced by at least $2|\gamma|/3 + 2$, i.e., violators are preserved.

Claim 2. *If γ is a simple cycle in a 3-colorable triangulation with interior triangulation T_γ and $\partial\gamma$ is the number of incidences of vertices of γ with black triangeles of T_γ, then*

- $\partial\gamma \geq |\gamma| - 3$ *if T_γ has no interior vertex, and*
- $\partial\gamma \geq 2|\gamma|/3$ *otherwise.*

Proof of Claim. We assume that all the faces of T_γ incident to an edge of γ are white. If not then adding white triangles to achieve this property increases $|\gamma|$ and keeps $\partial\gamma$ the same.

Suppose $\partial\gamma < |\gamma|$. Then on γ we find an *ear*, this is a vertex which has no incidence to a black triangle of T_γ, i.e., its degree in T_γ is 2.

We first deal with the case where T_γ has no interior vertex, i.e., all the edges not on γ are chords. If b is an ear and a, c are the neighbors of b on γ, then ac is an edge and, if $|\gamma| > 3$, there is a black triangle acx in T_γ. An ear is *reducible* if b has a neighbor on γ which is only incident to a single black triangle in T_γ. Assume that c is such a neighbor of b, then the second neighbor d of c on γ has an edge to x. delete b and c and identify a with d and also identify the edges xa and xd. This results in a cycle γ' with $|\gamma'| = |\gamma| - 3$. We call this an *ear reduction with center* x. Figure 8 (left and middle) shows sketches of reducible ears with

$x \in \gamma$. If $|\gamma| > 3$, then there is a reducible ear, otherwise the average degree of a vertex would be 4. This is impossible because T_γ has $2|\gamma| - 3$ edges.

If starting with γ we can perform m reductions, then $|\gamma| = 3m + 3$ and $\partial\gamma = 3m$. This completes the proof in this case.

Now assume that T_γ has an interior vertex. Again there is an ear b, let a, c be the neighbors of b on γ. Then a, c is an edge and there is a black triangle acx in T_γ. Now x may also be an inner vertex, see Figure 8 (right). However, if x is the unique common neighbor of a and d, then we can perform an *ear reduction with center* x by identifying a with d as well as the edges xa and xd. This results in a cycle γ' with $|\gamma'| = |\gamma| - 3$. Note that when x is not on γ we have $\partial\gamma = \partial\gamma' + 2$, while $\partial\gamma = \partial\gamma' + 3$ when x belongs to γ.

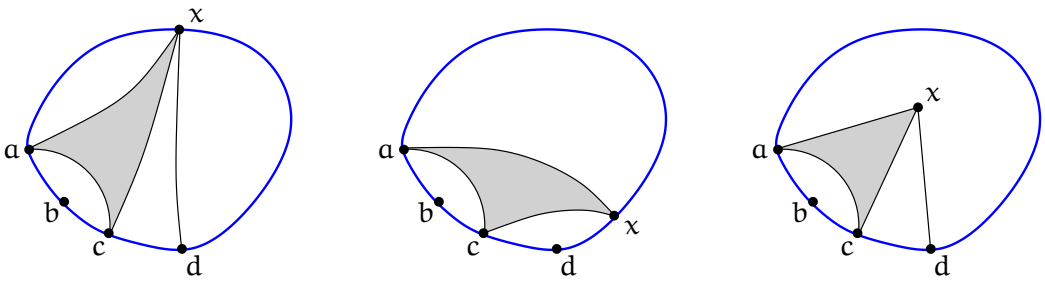

Figure 8: Three examples where b is a reducible ear.

If b is a reducible ear but a and d share several neighbors, then there is an extreme common neighbor y with the property that the cycle a, b, c, d, y encloses all the common neighbors of a and d. In this case we perform an ear reduction with center y (since a and d have the same color in every 3-coloring, the reduced graph remains 3-colorable and its faces 2-colorable). The reduction again yields a cycle γ' with $|\gamma'| = |\gamma| - 3$ and $\partial\gamma \geq \partial\gamma' + 2$.

After a series of m reductions we obtain a cycle γ' which has no reducible ear. Suppose that there remains an interior vertex in the triangulation $T_{\gamma'}$. Now every ear of $T_{\gamma'}$ has two neighbors which are incident to at least two black triangles. This shows that $\partial\gamma' \geq |\gamma'|$. Hence $\partial\gamma \geq \partial\gamma' + 2m \geq |\gamma'| + 2m = |\gamma| - 3m + 2m = |\gamma| - m$. Since $m \leq |\gamma|/3$ we arrive at $\partial\gamma \geq 2|\gamma|/3$.

Now suppose that $T_{\gamma'}$ has no interior vertex. There has been a last reduction where a and d had at least two common neighbors and the outermost y was on the current outer cycle γ^*. In this case one of the edges ay or dy is incident to a black triangle which disappears with the reduction (cf. Figure 10 (right)), hence, in this step $\partial\gamma^*$ drops by 4. For the initial γ we get: $|\gamma| = 3m + 3$ and $\partial\gamma \geq 2m + 2$. This completes the proof of the claim. △

We have already seen that the claim implies that we may assume that $g = 1$, i.e., the violator T_S only has a single big face, the outer face f_∞. We write $r_{f_\infty} = 3\rho$, the condition for violation becomes $\partial W < 2\rho + 2$.

Let γ be the boundary cycle of the unique big face. While the outer face of T has to be contained in the big face, we prefer to think of a drawing of T_S such that the big face is the interior of γ. It will be crucial, however, that in the inner triangulation of γ inherited from T there is a special black triangle δ_∞. The goal is to find a babet in the interior of γ. We use induction on ρ.

In the case $\rho = 1$ the triangle γ has $\partial W < 4$ incidences with black triangles from the inside. The unique configuration with this property is shown in Figure 9. Since the black triangle δ_∞ is not yet in the picture one of the triangles must be separating. If the separating triangle was

not the central one it would lead to an increase of ∂W. Hence the white central triangle is separating, i.e., a babet.

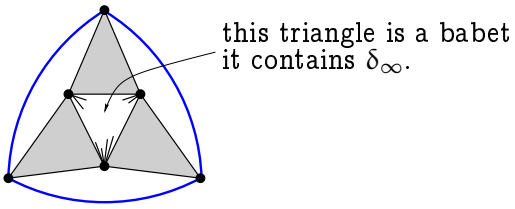

Figure 9: Illustration for the case $\rho = 1$.

Now let $\rho \geq 2$. Assuming a black incident triangle for every vertex of γ we obtain $\partial W \geq 3\rho \geq 2\rho + 2$. Therefore, on γ we find an *ear*. As above we aim for an ear reduction. Let b be a reducible ear with neighbors a and c such that c is only incident to a single black triangle acx inside γ and d is the second common neighbor of c and x. In the proof of Claim 2 we have seen that in this case a reduction is possible which preserves the violation inequality.

If x is the unique common neighbor of a and d, then the reduction leads to a decrease of ∂W by 2 or 3 and a decrease of ρ by 1, whence the reduced cycle remains violating.

If b is reducible but a and d share several neighbors, then we aim at a reduction whose center y is the extreme common neighbor of a and d. If this cycle does not enclose the black triangle δ_∞ we can apply the reduction with center y.

The described reductions may decrease ρ until it is 1 whence there is a babet. In fact we will complete the proof by showing that when no reduction is possible and $\rho > 1$, then the violator inequality is not fulfilled.

We first discuss the case where b is reducible but a and d share several neighbors and δ_∞ is enclosed in the cycle a, b, c, d, y where y is the extreme common neighbor of a and d. We show that in this case we can find a cycle γ' of length 6 which is a violator, i.e., $\partial\gamma < 6$.

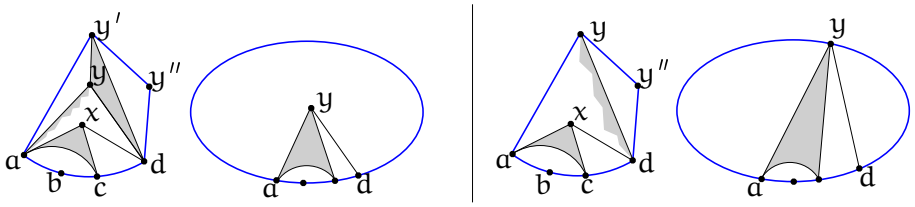

Figure 10: Illustration for the subconfigurations generated from a cycle a, b, c, d, y enclosing δ_∞.

Suppose y is in the interior of γ in this case we take the cycle a, b, c, d, y add a new common neighbor y' for a, d, y and an ear y'' over the black triangle containing y'. This yields a 6-cycle γ'' as shown in Figure 10 (left 1). In the interior of γ we replace the triangles inside a, b, c, d, y by the 3 triangles of a reducible ear, see Figure 10 (left 2) and refer to the cycle with the simplified interior as γ'. Now we compare $\partial\gamma$ with $\partial\gamma'$ and $\partial\gamma''$ and use the bound previously shown in the claim for γ', i.e., $\partial\gamma' \geq 2|\gamma'|/3 = 2|\gamma|/3$. Taking into account that on each of γ' and γ'' we see two incidences with black triangles which are not counted in $\partial\gamma$ we get $2|\gamma|/3 + 2 > \partial\gamma = (\partial\gamma'' - 2) + (\partial\gamma' - 2) \geq \partial\gamma'' + 2|\gamma|/3 - 4$. Hence $\partial\gamma'' < 6$, whence γ'' is also a violator.

If y is a vertex on the cycle γ we add a new ear y'' either over ay or over dy depending on which is incident to a black triangle. This yields a 6-cycle γ'' as shown in Figure 10 (right 1). In the interior of γ we replace the triangles inside a, b, c, d, y by the 3 triangles of a reducible ear, see Figure 10 (right 2) and refer to the cycle with the simplified interior as γ'. Taking into account that on γ' we see three incidences with black triangles which are not counted in $\partial\gamma$ we get $2|\gamma|/3 + 2 > \partial\gamma \geq \partial\gamma'' + (\partial\gamma' - 3) \geq \partial\gamma'' + 2|\gamma|/3 - 3$. Hence $\partial\gamma'' < 5$, whence γ'' is also a violator.

If $\rho \geq 3$ and there are no reducible ears, then both neighbors of each ear vertex have two incidences with black triangles. Let each vertex with at least two incidences with black triangles discharge $1/2$ to the neighbors, then all vertices have a weight of at least 1. We get $\partial W \geq 3\rho > 2\rho + 2$ and the example is not a violator.

For the case $\rho = 2$ we consider circular sequences $(s_1, s_2, s_3, s_4, s_5, s_6)$ with $\sum_i s_i < 2\rho+2 = 6$ such that there is an inner Eulerian triangulation of a 6-gon with only white triangles touching the 6-gon and s_i black incident triangles at vertex v_i of the 6-gon. A vertex v_i with $s_i = 0$ is an ear. Clearly, the circular sequence has no 00 subsequence. With two ears which share a neighbor of degree 1, i.e., with a 010 subsequence, we have the graph T_1 from Figure 11, this triangulation does not occur in our setting since it does not contain a black δ_∞ which is vertex disjoint from the outer 6-gon. Making any of the four triangles of T_1 separating so that it can accommodate δ_∞ in its interior would make $\sum_i s_i \geq 6$.

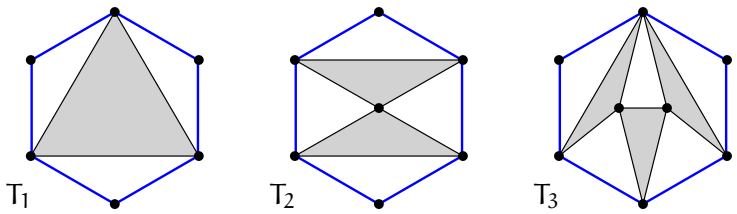

Figure 11: Three triangulations with $\rho = 2$ and $\partial W < 6$.

With a 0110 subsequence we have T_2. Again there is no δ_∞ in T_2 and making a triangle separating would make $\sum_i s_i \geq 6$. It remains to look at sequences without 00, and 010, and 0110 but $\sum_i s_i \leq 5$. The sequence 011102 is the unique sequence with these properties and there is a unique corresponding triangulation T_3. As with T_1 and T_2 there is no δ_∞ in T_3 and making a triangle separating would make $\sum_i s_i \geq 6$. □

3.1 Plattenbau Representations in the Babet-Free Case

Let T be a 3-colorable triangulation which has no babet. Due to Proposition 4 we find the α-orientation of H_T. This orientation can be represented on the dual T^* of T as a collection $\mathcal{C}$ of cycles such that every face which is not incident to v_∞ contains exactly one fragment of a cycle which leaves the face in distinct vertices of U° and every vertex of U° is covered by one of the cycles (Eppstein and Mumford [7] refer to this structure as *cycle cover*). The connected components of $\mathbb{R}^2 \setminus \mathcal{C}$ can be two-colored in white and pink such that the two sides of each cycle have distinct colors. The two-coloring is unique, if we want the unbounded region to be colored white. This two-coloring of the plane induces a partition of the vertices of U' into U'_w, U'_p where U'_w consists of all vertices living in white regions and U'_p consists of the vertices in pink regions, see Figure 12 for an example. An important property of the partition is that every vertex of $u \in U^\circ$ is adjacent to vertices from both classes U'_w and U'_p. This follows from

the fact that a cycle C from $\mathcal{C}$ contains u, whence two of the edges of u are on one side and the third is on the other side of C.

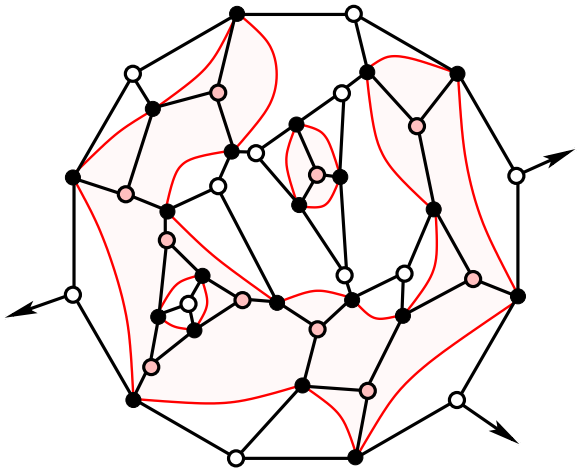

Figure 12: Example of a T^* with a cycle cover of U° and the induced partition of U'.

The partition U'_w, U°, U'_p of the vertices of $T^*\setminus\{v_\infty\}$ corresponds to the partition into minima, saddle points, maxima of the vertices of the orthogonal surface with skeleton T^*. To construct this orthogonal surface we first define a 3-connected planar graph G whose vertex set is U'_w, the edges of G are in bijection with U° and each bounded face of G contains exactly one vertex of U'_p. This graph G will be decorated with a Schnyder wood, i.e., an orientation of the edges which obeys the following rules:

(W1) On the outer face of G there are three special vertices a_r, a_g, a_b colored red, green, and blue in clockwise order. For $c \in \{r, g, b\}$ vertex a_c is equipped with an outward oriented half-edge of color c.

(W2) Every edge e is oriented in one or in two opposite directions. The directions of edges are colored such that if e is bioriented the two directions have distinct colors.

(W3) Every vertex v has outdegree one in each color $c \in \{r, g, b\}$. The edges e_r, e_g, e_b leaving v in colors r, g, b occur in clockwise order. Each edge entering v in color c enters v in the sector bounded by the two e_i with colors different from c (see Figure 13).

(W4) There is no interior face whose boundary is a directed cycle in one label.

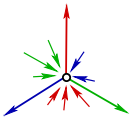

Figure 13: Illustration for the vertex condition (W3).

The construction of G and the Schnyder wood S is in several steps. Consider a 3-coloring of T with colors r, g, b, such that on the outer triangle these colors appear clockwise in the given order. Note that this implies that all white triangles see r, g, b in clockwise order and all black

triangles see r, g, b in counterclockwise order. The coloring of T induces a 3-coloring of the edges: for edge $e = v, v'$ use the unique color which is not used for v and v'. This edge-coloring of T can be copied to the dual edges. This yields an edge-coloring of T^* such that each vertex in U' is incident to edges of colors r, g, b in clockwise order. Delete v_∞ from T^* but keep the edges incident to v_∞ as half edges at their other endpoint, we denote the obtained graph as T^*_∞. The neighbors of v_∞ are the special vertices a_r, a_g, a_b for the Schnyder wood.

Next we introduce some new edges. For every black vertex $u \in U^\circ$ which is adjacent to only one vertex white vertex v of U'_w we identify the unique face f which is adjacent to u but not to v. Connect u to a vertex v' on the boundary of f which belongs to U'_w. Note that the edge uv' is intersected by a cycle from $\mathcal{C}$ and that both faces obtained by cutting f via u, v' contain the vertex $v' \in U'_w$. This shows that we can add edges to all vertices of U° which are adjacent to only one vertex in U'_w without introducing crossings. The color of vu is copied to the new edge uv'. Figure 14 exemplifies the coloring of T^*_∞ together with the additional edges.

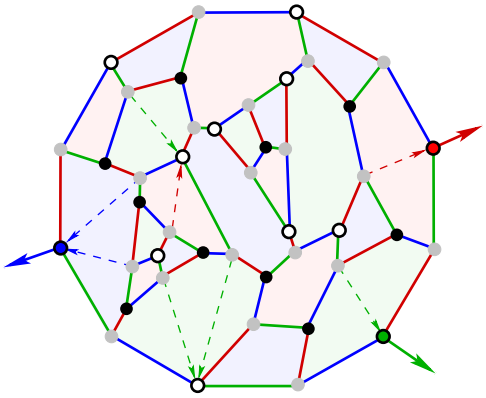

Figure 14: The coloring of the edges of T^*_∞ obtained from the 3-coloring of T. The dashed arrows are the additional edges.

Now remove all the edges incident to vertices in U'_p. In the remaining graph all the vertices of U° are of degree 2. We remove these 'subdivision' vertices and melt the two edges into one. The result is G. We claim that orienting the three edges of $v \in U'_p$ which come from an edge of T^*_∞ as outgoing we obtain a Schnyder wood of G. Indeed (W1), (W2), and (W3) follow directly or from what we have already said. For (W4) we need a little argument. Consider a monochromatic edge vv' and let f be one of the faces of G containing this edge on the boundary. The other edge on the boundary of f which contains v' is either incoming in the same color or outgoing in a different color. This shows that there is no monochromatic directed facial cycle containing vv'. Now consider a face f of G which has no monochromatic edge. Note that f is a union of faces of T^*_∞ and each face of T^*_∞ is incident to a pink vertex in U'_p. Let $w \in U'_p$ be a vertex in the interior of f such that in T^*_∞ there is an edge wu with $u \in U^\circ$ on the boundary ∂f of f. Let $c \in \{r, g, b\}$ be the color of the edge wu. Vertex u has two neighbors v, v' on ∂f. By looking at the colors of edges of T^*_∞ we see that at v and v' the incident edge on ∂f which is different from vv' has color c. In the Schnyder wood we therefore see these outgoing in color c at v and v' one of them being oriented clockwise, the other counterclockwise on the boundary of f. This shows that ∂f supports no monochromatic directed cycle.

For the following we rely on the theory of Schnyder woods for 3-connected planar graphs, see e.g. [8] or [15] or [10]. In the Schnyder wood S on G for every vertex v and every color $c \in$

$\{r, g, b\}$ there is a directed path $P_c(v)$ of color c from v to a_c. The three paths $P_r(v), P_g(v), P_b(v)$ pairwise only share the vertex v. The three paths of v partition the interior of G into 3 regions. For $\{c_1, c_2, c_3\} = \{r, g, b\}$ we let $R_{c_1}(v)$ be the region bounded by P_{c_2} and P_{c_3}. With v we associate the region vector (v_r, v_g, v_b) where v_c is the number of faces of G in region $R_c(v)$. Figure 14 illustrates regions and region vectors.

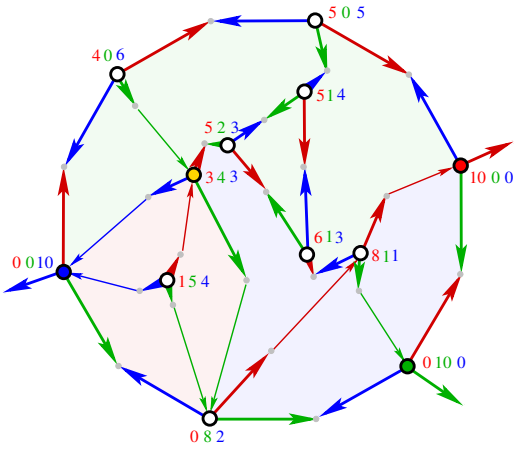

Figure 15: A Schnyder wood with a shading indicating the regions of the yellow vertex. Vertices are labeled with their region vector.

Let $\mathcal{V} = \{(v_r, v_g, v_b) : v \in V(G)\}$ be the generating set for an orthogonal surface $\mathfrak{S}$. In slight abuse of notation we identify region vectors with their corresponding vertices and say that $\mathfrak{S}$ is generated by $V(G)$. The minima of $\mathfrak{S}$ are the vertices of G. Moreover, $\mathfrak{S}$ supports the Schnyder wood S in the sense that every outgoing edge at v in S corresponds to an edge of the skeleton of $\mathfrak{S}$ such that the direction of the skeleton edge is given by the color of the edge. In fact from the clockwise order of directions of skeleton edges at minima, saddle points and maxima it can be concluded that the skeleton $G_{\mathfrak{S}}$ of $\mathfrak{S}$ is T^*. With Proposition 3 we obtain a Plattenbau representation of T.

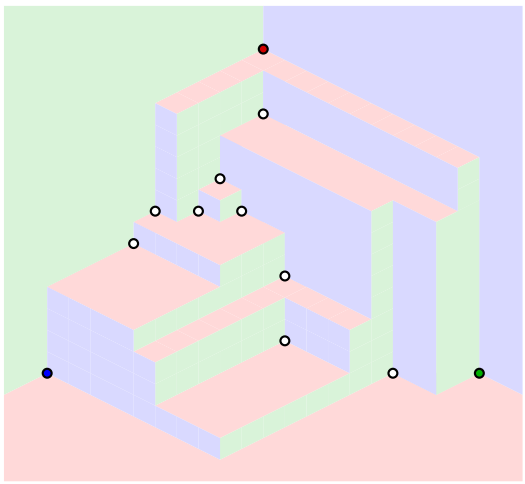

Figure 16: The orthogonal surface obtained from the region vectors given in Figure 15.

Since the set of α-orientations of a fixed planar graph carries the structure of a distributive lattice [10], and we have shown a correspondence of such a set with the orthogonal surfaces with given skeleton, we obtain:

Corollary 5. *Let* G *be a planar cubic bipartite graph with specified vertex* v_∞ *such that the dual triangulation is babet-free. The set of orthogonal surfaces with skeleton* G *and vertex* v_∞ *at infinity carries a distributive lattice structure.*

3.2 Plattenbau Representations in the Presence of Babets

Let T be a 3-colorable triangulation, suppose that T contains babets. Being separating triangles babets can be nested, let $\mathcal{B}$ be the family of basic babets of T, i.e., of babets which are not contained in the interior of another babet. Let $T_\triangle$ be the triangulation obtained from T by cleaning all the babets, i.e., removing the interior vertices and their incident edges from all babets $B \in \mathcal{B}$. Clearly $T_\triangle$ is 3-colorable and babet-free. Triangles which have been babets are black. With the method from the previous subsection we get an orthogonal surface $\mathfrak{S}_\triangle$ for $T_\triangle$. In this representation triangles which have been babets correspond to saddle points. For later reference let u_B be the saddle point corresponding to $B \in \mathcal{B}$.

For each babet $B \in \mathcal{B}$ let T_B the inside triangulation of B in T. Clearly, T_B is 3-colorable, hence, its triangles can be colored black and white with the outer face being black (note that this coloring of T_B is obtained from the coloring of triangles in T by exchanging black and white). Assuming that T_B has no babet we obtain an orthogonal surface $\mathfrak{S}_B$ for T_B.

The construction of the orthogonal surface $\mathfrak{S}_B$ works with the assumption that the vertices of the outer face, i.e., of the triangle B are colored r, g, b in clockwise order. The same assumption for the full triangulation T implies that the vertices of B are colored r, b, g in clockwise order.

The goal is to patch $\mathfrak{S}_B$ at the saddle point u_B to $\mathfrak{S}_\triangle$ so that the flats corresponding to a vertex of B in the two orthogonal surfaces are coplanar. Let f_r, f_g, and f_b be the red, green and blue flat at u_B in $\mathfrak{S}_\triangle$, they represent the vertices v_r, v_g, v_b of B with their color in T. At u_B exactly one of the three flats has a concave angle, we assume that this flat is f_r, the other cases are completely symmetric. The point u_B is an interior point of the rectangle $R = R(f_r)$ spanned by the extreme points of f_r. The point u_B is the apex of a convex corner whose sides coincide locally with $R \setminus f_r$, f_g and f_b. In this corner we see the colors of the flats in clockwise order as r, b, g. Hence, we can patch and appropriately scaled down copy of $\mathfrak{S}_B$ into this corner such that the red outer flat of $\mathfrak{S}_B$ becomes part of $R \setminus f_r$, while the green outer flat of $\mathfrak{S}_B$ becomes part of f_b and the blue outer flat of $\mathfrak{S}_B$ becomes part of f_g. With the technique of Proposition 3 we obtain a rectangle contact representation of the subgraph of T induced by all the vertices of T which are represented by flats of $\mathfrak{S}_\triangle$ and $\mathfrak{S}_B$. See Figure 17 for an illustration.

Repeating the procedure for further babets in $\mathcal{B}$ and for babets which may occur in triangulations T_B we eventually obtain an rectangle contact representation of T. This completes the proof of Theorem 1.

3.3 Comments on Related Work

Eppstein and Mumford [7] study orthogonal polytopes and their graphs. They define *corner polyhedra* as polytopes obtained from what we call an orthogonal surface by restricting the surface to the bounded flats and connecting their boundary to the origin $\mathbf{0} = (0, 0, 0)$, this replaces the 3 unbounded flats of an orthogonal surface by three flats closing the polytope.

corner polyhedra

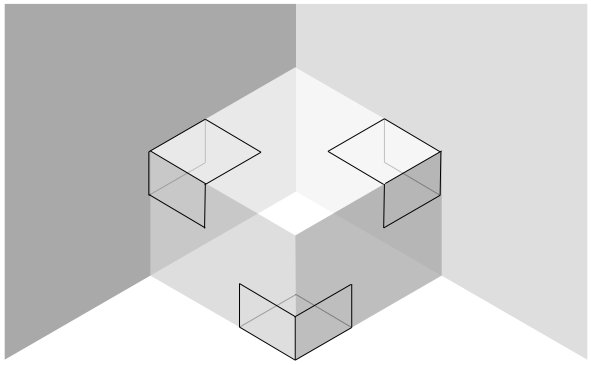

Figure 17: An orthogonal surface with three saddle points. The frames indicate how to patch a small orthogonal surfaces at the respective saddle points.

Eppstein and Mumford show that the skeleton graphs of corner polyhedra are exactly the cubic bipartite 3-connected graphs with the property that every separating triangle of the planar dual graph has the same parity. This is equivalent to our characterization of these graphs as duals of 3-colorable triangulations with admit a choice of the outer face such that there are no babets, see Proposition 4.

A major part of their proof is devoted to the construction of a rooted cycle cover, respectively, to the investigation of necessary and sufficient conditions for the existence of such a cycle cover. The proof is based on a set of operations that allow any 4-connected Eulerian triangulation to be reduced to a smaller one. In contrast we show the equivalent existence of an α-orientation with a counting argument. Given a cycle cover Eppstein and Mumford provide a construction of an appropriate orthogonal surface from the combinatorial data by combining the coordinates obtained from plane drawings of three orthogonal projections. In contrast we refer to the established theory of Schnyder woods and their relation to orthogonal structures to get the results.

xyz polyhedra

As a more general class than corner polyhedra Eppstein and Mumford define *xyz polyhedra* as orthogonal polytopes with the property that each axis-parallel line through a vertex contains exactly one additional vertex. They characterize the skeletons of them as cubic bipartite 3-connected graphs, i.e., as the duals of 3-colorable triangulations. Modulo the 'reflection' of the three outer flats this corresponds to our Theorem 1. The main step in the proof is the gluing of an orthogonal surface into a corner of another orthogonal surface, see Section 3.2 and also Fig. 29 in [7].

TC-scheme

A recent paper of Gonçalves [18] can be used as a basis for yet another proof of Theorem 1, i.e., a proof of the characterization of xyz polyhedra. Gonçalves uses a system of linear equations to construct a *TC-scheme* (triangle contact scheme) for a given 3-colorable triangulation. The TC-scheme comes very close to a segment contact representation with segments of 3 slopes for the input graph, however, there can be degeneracies: segments may degenerate to points (this relates to babets) and segments ending on two sides of another segment may have coinciding endpoints. The TC-scheme can be transformed into an orthogonal surface. First adjust the directions to have slopes 0, $+\frac{\pi}{3}$, and $-\frac{\pi}{3}$, then add an orthogonal peak in each gray triangle[5] and an orthogonal valley in each white triangle, and extend the outer flats.

[5] This refers to the two color classes of the triangles of the TC-scheme, not to the two classes of triangles of the original triangulation.

This yields an orthogonal surface. If there are no degeneracies the orthogonal surface properly represents the triangulation via flat contacts. Degeneracies of the TC-scheme translate into corners of degree 6 in the orthogonal surface, they can be resolved by *shifting flats* (c.f. [15] for details on flat shifting). Finally as in the other two approaches babets have to be recovered by patching their orthogonal surface into corners of the surface.

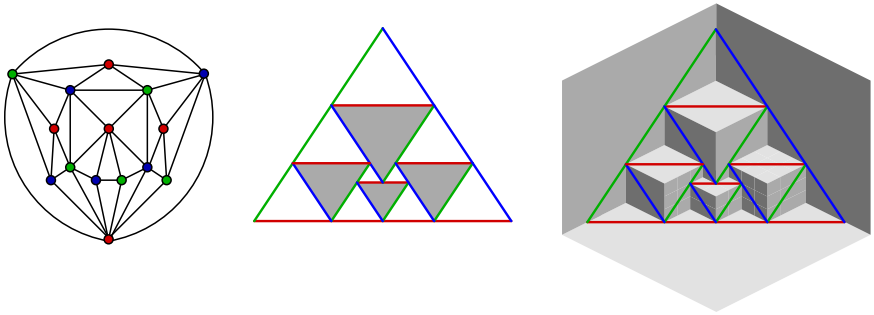

Figure 18: A 3-colored triangulation, a TC-scheme of the triangulation and the corresponding orthogonal surface.

A nice aspect of this approach is that the partition of white triangles of the triangulation into peak and valley triangles is done by solving the linear system, no need of computing an α-orientation or a cycle cover for this task.

4 Generic Boxed Plattenbauten and Octahedrations

In this section we characterize the touching graphs of generic boxed Plattenbauten, that is, we prove Theorem 2. Furthermore, we provide iterative constructions for generic boxed Plattenbauten from smaller ones in Subsection 4.1. Here is the theorem again.

Theorem 2. *A graph G is the touching graph of a generic boxed Plattenbau $\mathcal{R}$ if and only if there are six outer vertices in G such that each of the following holds:*

(P1) *G is connected and the outer vertices of G induce an octahedron.*

(P2) *The edges of G admit an orientation such that*

- *the bidirected edges are exactly the outer edges,*
- *each vertex has exactly 4 outgoing edges.*

(P3) *The neighborhood $N(v)$ of each vertex v induces a spherical quadrangulation $SQ(v)$ in which the out-neighbors of v induce a 4-cycle.*

- *If v is an outer vertex, this 4-cycle bounds a face of $SQ(v)$.*

(P4) *For every edge uv of G with common neighborhood $C = N(u) \cap N(v)$, the cyclic ordering of C around u in $SQ(v)$ is the reverse of the cyclic ordering of C around v in $SQ(u)$.*

First, as noted earlier, in a generic Plattenbau for any two touching rectangles R, R' one rectangle, say R uses part of one of its edges for this incidence and does not use this edge for

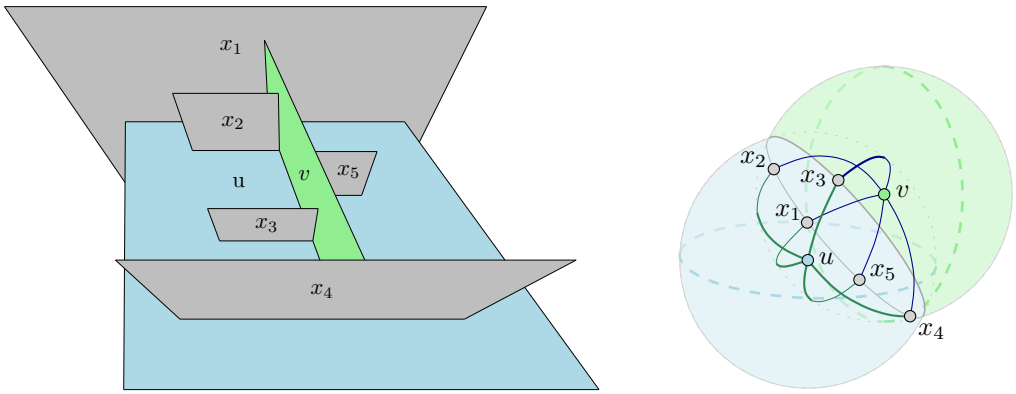

Figure 19: Two rectangles (green and blue) and their common neighborhood.

any other incidence. We denote this as $R \to R'$ and remark that this orientation has already been used in the proof of Observation 2.

Second, in any generic boxed Plattenbau $\mathcal{R}$ there are six rectangles that are incident to the unbounded region. We refer to them as *outer rectangles* and to the six corresponding vertices in the touching graph G for $\mathcal{R}$ as the *outer vertices*. The corners incident to three outer rectangles are the *outer corners*, and the inner regions/cells of $\mathcal{R}$ will be called *rooms*.

outer rectangles
outer corners
rooms

Whenever we have specified some vertices of a graph to be outer vertices, this defines inner vertices, outer edges, and inner edges as follows: The *inner vertices* are exactly the vertices that are not outer vertices; the *outer edges* are those between two outer vertices; the *inner edges* are those with at least one inner vertex as endpoint. We shall use these notions for a Plattenbau graph, as well as for some planar quadrangulations we encounter along the way.

Let us start with the necessity of Items (P1) to (P4) in Theorem 2.

Proposition 6. *Every touching graph of a generic boxed Plattenbau satisfies Items (P1) to (P4) in Theorem 2.*

Proof. Item (P1) follows directly from the definition of boxed Plattenbauten. Also, for Item (P2) simply orient each edge towards the end-vertex whose rectangle has interior points in the intersection. This way, any edge between two outer vertices is bidirected, which is in accordance with Item (P2). Now, Item (P3) follows from Observation 1 Item 2 together with the fact that edge-maximal planar bipartite graphs are quadrangulations. Indeed, if the rectangles on one side of a given rectangle would not induce a quadrangulation, then there would be a rectangle with a free edge and $\mathcal{R}$ would not be boxed. Let us finally argue Item (P4). The common neighbors of two vertices u, v lie on the circle that is the intersection of the spheres $SQ(u)$ and $SQ(v)$ with centers u and v, respectively. Since u and v are on different sides of the intersection, u, v see the vertices on the circle in opposite order. See Figure 19 for an illustration. □

Next, we prove the sufficiency in Theorem 2, i.e., for every graph G satisfying Items (P1) to (P4) we find a generic boxed Plattenbau with touching graph G.

Fix a graph $G = (V, E)$ with six outer vertices and edge orientation fulfilling Items (P1) to (P4). For each vertex $v \in V$ denote by $SQ(v)$ the spherical quadrangulation induced by $N(v)$ given in Item (P3). By Item (P3), the out-neighbors of vertex v induce a 4-cycle in $SQ(v)$, which we call the *equator* O_v of $SQ(v)$. The equator O_v splits the spherical quad-

equator

rangulation $SQ(v)$ into two *hemispheres*, each being a plane embedded quadrangulation with outer face O_v with the property that each vertex of $SQ(v) - O_v$ is contained in exactly one hemisphere. The vertices of O_v are the outer vertices of either hemisphere. Note that one hemisphere (or even both) may be trivial, namely when the equator bounds a face of $SQ(v)$. *hemispheres*

We proceed with a number of claims.

Claim 3. *In each hemisphere, each inner vertex has exactly two outgoing edges and no outer vertex has an outgoing inner edge.*

Proof of Claim. Let u be any inner vertex of a hemisphere of $SQ(v)$. We shall first show that u has at least two out-neighbors in that hemisphere. We have $u \in N(v) - O_v$, i.e., u is a neighbor of v but not an out-neighbor. Hence, the edge uv is directed from u to v and v lies on the equator O_u of $SQ(u)$. As such, v has two neighbors w_1, w_2 on the equator of O_u, i.e., w_1, w_2 are out-neighbors of u. Also $w_1, w_2 \in SQ(v)$ since they are neighbors of v. Hence, u has at least two out-neighbors in $SQ(v)$ and, by planarity of $SQ(v)$, these are in the same hemisphere as u, as desired.

Finally, each hemisphere of v is a plane quadrangulation with outer 4-cycle O_v, and as such has exactly $2k$ inner edges for k inner vertices. As each inner vertex has at least two outgoing edges, the edge count gives that each inner vertex has exactly two outgoing edges. Moreover, each inner edge is outgoing at some inner vertex, i.e., no outer vertex of the hemisphere has an outgoing inner edge. △

Together with v each equator edge of $SQ(v)$ induces a triangle in G. These four triangles are the *equator triangles* of v. *equator triangles*

Claim 4. *Every triangle in G is an equator triangle.*

Proof of Claim. Let Δ be a triangle in G with vertices u, v, w. First, we shall show that Δ is not oriented as a directed cycle, i.e., Δ has a vertex of out-degree two. Without loss of generality let uv be directed from u to v. If uw is directed from u to w, we are done. So assume that uw is directed from w to u. Then $u \in N(v) - O_v$ is an inner vertex of a hemisphere of $SQ(v)$. Moreover $w \in N(v)$ has an outgoing edge to u, and Claim 3 implies that w is an inner vertex of the same hemisphere of $SQ(v)$. In particular, vw is directed from w to v whence w is a vertex of out-degree two in Δ.

Now let a be the vertex in Δ with out-degree two and b, c be its out-neighbors in Δ. Then b and c lie on the equator of a and are connected by an edge bc in G. Thus Δ is an equator triangle. △

Clearly, a vertex w forms a triangle with two vertices u and v if and only if uv is an edge and w is a common neighbor of u and v. Equivalently, w is adjacent to v in $SQ(u)$, which in turn is equivalent to w being adjacent to u in $SQ(v)$. Hence, the set $N(u) \cap N(v)$ of all common neighbors (and thus also the set of all triangles sharing edge uv) is endowed with the clockwise cyclic ordering around v in $SQ(u)$, as well as with the clockwise cyclic ordering around u in $SQ(v)$. By Item (P4), these two cyclic orderings are reversals of each other.

Let us define for a triangle Δ in G with vertices u, v, w the two *sides* of Δ as the two cyclic permutations of u, v, w, which we denote by $[u, v, w]$ and $[u, w, v]$. So triangle Δ has the two sides $[u, v, w] = [v, w, u] = [w, u, v]$ and $[u, w, v] = [w, v, u] = [v, u, w]$. We define a binary *sides* $[u, v, w]$

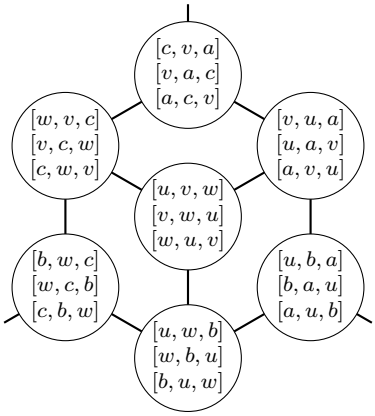

Figure 20: The second neighborhood of vertex $[u, v, w]$ in the auxiliary graph H.

relation $\sim$ on the set of all sides of triangles in G as follows.

$$[u, v, a] \sim [v, u, b] \text{ if } \begin{cases} a \text{ comes immediately before } b \\ \text{in the clockwise cyclic ordering} \\ \text{of } N(u) \cap N(v) \text{ around } v \text{ in } SQ(u) \end{cases} \tag{1}$$

Note that by (P4) a comes immediately before b in the clockwise ordering around v if and only if b comes immediately before a in the clockwise ordering around u. Thus $[u, v, a] \sim [v, u, b]$ also implies $[v, u, b] \sim [u, v, a]$, i.e., $\sim$ is a symmetric relation and as such encodes an undirected graph H on the sides of triangles.

Claim 5. *Each connected component of* H *is a cube. The corresponding subgraph in* G *is an octahedron.*

Proof of Claim. Consider any fixed vertex $[u, v, w]$ of H. Then vw is an edge of G contained in $SQ(u)$. As $SQ(u)$ is a quadrangulation, vertex v has degree at least two in $SQ(u)$. Hence, there exists a unique vertex a in $SQ(u)$ such that $[u, v, w] \sim [v, u, a]$ according to Eq. (1). Moreover, a and w are both neighbors of v in $SQ(u)$ and hence non-adjacent in G, i.e., $a \in (N(u) \cap N(v)) - N(w)$. Symmetrically, we find $b \in (N(w) \cap N(u)) - N(v)$ with $[w, u, v] \sim [u, w, b]$ and $c \in (N(v) \cap N(w)) - N(u)$ with $[v, w, u] \sim [w, v, c]$. It follows that a, b, c are pairwise distinct vertices of G and thus $[u, v, w]$ has degree exactly three in H.

Now recall that vw is an edge of G contained in $SQ(u)$. Consider the face f in $SQ(u)$ for which v comes immediately before w in the clockwise ordering around f. Let v, w, s, t be the clockwise ordering of vertices around f. Then, for example, w comes immediately before t in the clockwise cyclic ordering around v in $SQ(u)$. Using Eq. (1), we have the following.

$$[u, v, w] \sim [v, u, t] = [u, t, v] \sim [t, u, s] = [u, s, t] \sim [s, u, w] = [u, w, s] \sim [w, u, v] = [u, v, w]$$

It follows that $t = a$ and $s = b$. I.e., the component of H with vertex $[u, v, w]$ contains the four triangle sides $[u, v, w]$, $[u, w, b]$, $[u, b, a]$, $[u, a, v]$ and these form a 4-cycle in H. As v, w, a, b are pairwise distinct vertices in G, we have $[u, v, w] \not\sim [u, b, a]$ and $[u, w, b] \not\sim [u, a, v]$, meaning that the above 4-cycle in H is induced.

Repeating the same argument for $[v, w, u]$ in quadrangulation $SQ(v)$ and $[w, u, v]$ in quadrangulation $SQ(w)$, we get the induced 4-cycles

$$[v, w, u] \sim [w, v, c] = [v, c, w] \sim [c, v, a] = [v, a, c] \sim [a, v, u] = [v, u, a] \sim [u, v, w] = [v, w, u]$$

and

$$[w, u, v] \sim [u, w, b] = [w, b, u] \sim [b, w, c] \\ = [w, c, b] \sim [c, w, v] = [w, v, c] \sim [v, w, u] = [w, u, v].$$

As $[u, v, w] = [v, w, u] = [w, u, v]$, these three induced 4-cycles in H pairwise share exactly one edge, as shown in Figure 20. For each of the three vertices $[a, c, v]$, $[b, a, u]$, and $[c, b, w]$, the third neighbor in H is yet to be explored. However by symmetry, each of those vertices is also in exactly three induced 4-cycles, which implies that they have the same third neighbor: vertex $[a, b, c] = [b, c, a] = [c, a, b]$.

Thus, the component of H containing $[u, v, w]$ is a cube. The eight corresponding triangles in G form an octahedron with vertex set $\{u, v, w, a, b, c\}$. △

With Claim 5 we have identified a family of octahedra in G such that each side of each triangle in G is contained in exactly one octahedron. We call these octahedra the *cells* of G, as these correspond in the 2-dimensional case to the 4-cycles bounding faces of the quadrangulation. As Eq. (1) puts two triangle sides $[u, v, a]$ and $[v, u, b]$ into a common cell if and only if the edges va and vb bound the same facial 4-cycle in $SQ(u)$, we have the following correspondence between the cells of G and the faces in the spherical quadrangulations. *cells*

Claim 6. *If $O \subseteq G$ is a cell of G and C is an induced 4-cycle in O, then C bounds a face of $SQ(v)$ and a face of $SQ(u)$ for the two vertices $u, v \in O - C$. Conversely, if C is a 4-cycle bounding a face of $SQ(v)$, then there is a cell O of G containing $\{v\} \cup V(C)$.*

Having identified the cells, we can now construct a generic boxed Plattenbau for G by identifying two opposite vertices in a particular cell, calling induction, and then splitting the rectangle corresponding to the identification vertex into two. The cells of G will then correspond to the rooms in $\mathcal{R}$, except that one cell of G will correspond to the unbounded region of $\mathcal{R}$ (which is not a room). To this end, we prove the following stronger statement:

Lemma 7. *Let G be a graph satisfying Items (P1) to (P4) and let A, B, C be three outer vertices forming a triangle in G. Then there exists a generic boxed Plattenbau $\mathcal{R}$ whose touching graph is G such that each of the following holds.*

(I1) The six outer vertices of G correspond to the outer rectangles of $\mathcal{R}$.

(I2) The cells of G correspond to the rooms of $\mathcal{R}$, except for one cell that is formed by all six outer vertices.

(I3) For any two vertices u, v with corresponding rectangles R_u, R_v we have $u \to v$ in the orientation of G if and only if $R_u \cap R_v$ contains an edge of R_u.

(I4) For each vertex v corresponding to a rectangle R_v, the rectangles touching R_v come in the same spherical order as their corresponding vertices in $SQ(v)$.

Proof. We proceed by induction on the number of vertices in $G = (V, E)$. As the base case we have $|V| = 6$ and $G \cong K_{2,2,2}$ is just an octahedron. In this case G has exactly eight triangles and 16 sides of triangles. There are exactly two cells, each isomorphic to G. The desired Plattenbau $\mathcal{R}$ is given by the six sides of an axis-aligned cuboid in $\mathbb{R}^3$. It is easy to see that $\mathcal{R}$ has the required properties.

So let us assume that $|V| > 6$, i.e., there is at least one inner vertex. Consider the three outer vertices A, B, C, which form a triangle in G. We shall first show that at least one of the quadrangulations $SQ(A)$, $SQ(B)$, $SQ(C)$ has an inner vertex. As G is connected by Item (P1), there is an edge in G from some inner vertex v to some outer vertex w with w not necessarily in $\{A, B, C\}$. Then v is an inner vertex of $SQ(w)$, i.e., one hemisphere of $SQ(w)$ is a plane quadrangulation with at least five vertices whose outer 4-cycle consists of four outer vertices of G. One edge of the outer 4-cycle has both endpoints in $\{A, B, C\}$ and, as there is some inner vertex, at least one of these two endpoints has an inner vertex as a neighbor.

So we may assume that A has an inner neighbor, i.e., the non-trivial hemisphere Q of $SQ(A)$ has an inner face f that is bounded by the edge BC and at least one inner vertex of G. Consider the cell O of G that contains all vertices on f, as given by Claim 6. Let the vertices of this octahedron O be denoted by A, B, C, a, b, c with the three pairs of non-adjacent vertices being $\{A, a\}$, $\{B, b\}$, and $\{C, c\}$. Note that at least one of a, b, c is in inner vertex of G since O includes an inner vertex of Q. In any case, vertices a, b, c form a triangle in G and each of the three vertices has outgoing edges to two of A, B, C. By Claim 4, one of a, b, c, say c, has outgoing edges to the other two vertices (a and b in this case). In particular, c is an inner vertex, as otherwise c has only outer vertices as out-neighbors (by Item (P2)), contradicting that one of a, b, c is an inner vertex.

Now we identify vertices c and C in G, denoting the resulting vertex by $\tilde{C}$ and the resulting graph by $\tilde{G}$. Each of A, B, a, b is a neighbor of c and C in G. We remove double edges during the identification, so that in $\tilde{G}$ vertex $\tilde{C}$ is connected to each of A, B, a, b with a single edge. In $\tilde{G}$ we choose the same six vertices except for $\tilde{C}$ replacing C as the outer vertices. We claim that $\tilde{G}$ together with this choice of outer vertices has the properties in Items (P1) to (P4). Indeed Item (P1) holds because each neighbor w of $\tilde{C}$ in $\tilde{G}$ that is not a neighbor of C in G has in G an incoming edge to c. In particular, such w is an inner vertex, as c is an inner vertex. Hence the outer vertices in $\tilde{G}$ induce an octahedron. Connectivity of $\tilde{G}$ follows from connectivity of G.

For Item (P2) we first prove the following.

Claim 7. *We have* $N(c) \cap N(C) = \{A, B, a, b\}$.

Proof of Claim. Suppose for the sake of contradiction that v is a common neighbor of c and C different from A, B, a, b. Then C and c are out-neighbors of v, i.e., v is a non-equator vertex in $SQ(c)$ and $SQ(C)$. Let w be an out-neighbor of v different from c, C. Then, by Claim 3 w is contained in $SQ(c)$ and $SQ(C)$, too. If w is neither on the equator of $SQ(c)$ nor on the equator of $SQ(C)$, we can repeat the argument with w taking the role of v. Thus assume that w is an out-neighbor of at least one of c, C. As out-neighbors of the outer vertex C are outer vertices, it follows that w is an out-neighbor of c, i.e., $w \in \{A, B, a, b\}$. By symmetry, assume that $w \in \{B, b\}$. Now consider the hemisphere Q of $SQ(w)$ that contains v as an inner vertex. As A, B, C, a, b, c form a cell, the vertices A, C, a, c form a quadrangular face in Q by Claim 6. Moreover, we know that c has outgoing edges to A and a, while v has outgoing edges to c and C, see Figure 21 for an illustration of the situation on $SQ(w)$.

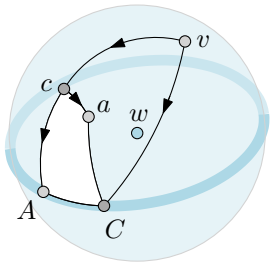

Figure 21: The situation in Claim 7 that leads to a contradiction.

Vertices a, A, c, C, and v induce a $K_{2,3}$ in $SQ(w)$. Since a, A, c, C bound a face of the hemisphere Q of $SQ(w)$, and A, C are outer vertices of G (hence outer vertices of Q), it follows that vertex a lies inside the 4-cycle K formed by A, c, v, C in Q. As Q is a quadrangulation, the 4-cycle K together with the vertices in its interior is as well a quadrangulation J with outer face K. Hence, J has $|V(J)|-4$ inner vertices and $2|V(J)|-8$ inner edges. One of the inner edges of J, namely the edge ca, is outgoing at the outer vertex c of J. Hence at most $2|V(J)|-9$ inner edges of J are outgoing at an inner vertex of J. But this is a contradiction to Claim 3, which states that each of the $|V(J)|-4$ inner vertices has exactly two outgoing edges in Q. △

Claim 7 implies that the orientation of G given by Item (P2) naturally induces an orientation of $\tilde{G}$ satisfying again Item (P2).

Claim 8. *Item (P3) holds for* $\tilde{G}$.

Proof of Claim. We shall show that for each vertex v of $\tilde{G}$, the neighborhood of v induces a spherical quadrangulation $SQ(v)$ in which the out-neighbors of v form a 4-cycle. We distinguish different cases of v and how $N(v)$ changes during the identification of c and C. For $v = \tilde{C}$, $N(v)$ in $\tilde{G}$ is the union of $N(c)$ and $N(C)$ in G. As A, B, C, a, b, c form a cell, A, B, a, b form a face in both $SQ(c)$ and $SQ(C)$ by Claim 6. Moreover, A, B, a, b are the equator in $SQ(c)$. Hence, the subgraph of $\tilde{G}$ induced by $N(v) = N(c) \cup N(C)$ can be obtained by pasting $SQ(c)$ into the face A, B, a, b of $SQ(C)$. This is a quadrangulation and the out-neighbors of $\tilde{C}$ are the same as for C, i.e., induce a 4-cycle. For $v \in \{A, B, a, b\}$, identifying C and c corresponds to merging opposite vertices of a face f in $SQ(v)$. As $N(c) \cap N(C) = \{A, B, a, b\}$ by Claim 7, in $SQ(v)$ vertices c and C have no common neighbor outside of f. Thus the identification of C and c in $SQ(v)$ preserves the property of being a quadrangulation and does not affect the equator. For $v \notin \{\tilde{C}, A, B, a, b\}$ the neighborhood of v does not change, except for possibly renaming c or C to $\tilde{C}$. This shows that $\tilde{G}$ satisfies Item (P3). △

Claim 9. *Item (P4) holds for* $\tilde{G}$.

Proof of Claim. Recall that during the identification of c and C, we changed the embedding of $SQ(v)$ only for $v \in \{\tilde{C}, A, B, a, b\}$. Thus we need to check only those edges in $\tilde{G}$ with at least one endpoint in $\{\tilde{C}, A, B, a, b\}$. First consider an edge $\tilde{C}v$ with $v \notin \{A, B, a, b\}$. If v was a neighbor of c in G, then in $SQ(\tilde{C})$ vertex v is embedded inside the quadrangle A, B, a, b. If v was a neighbor of C in G, then in $SQ(\tilde{C})$ vertex v is embedded outside the quadrangle A, B, a, b. By planarity of $SQ(\tilde{C})$, there is no edge between these two types of vertices. Thus the common neighborhood of $\tilde{C}$ and any $v \notin \{A, B, a, b\}$ coincides with either $N(c) \cap N(v)$ or $N(C) \cap N(v)$ in G. Say v was a neighbor of c. As the clockwise cyclic ordering around v in

$SQ(\tilde{C})$ is the same as in $SQ(c)$, and the clockwise ordering around $\tilde{C}$ in $SQ(v)$ is the same as that around c in $SQ(v)$ before, Item (P4) is satisfied here. The case of an edge $\tilde{C}v$ with $v \in \{A, B, a, b\}$ and the other cases are similar. △

Up to now we have shown that the graph $\tilde{G}$ obtained from G by identifying c and C satisfies Items (P1) to (P4). Thus, by induction there is a generic boxed Plattenbau $\mathcal{R}'$ whose touching graph is $\tilde{G}$ such that Items (I1) to (I4) hold. In particular the rectangles R_A, R_B, R_a, R_b for the 4-cycle A, B, a, b in $SQ(\tilde{C})$ enclose a rectangular region in one corner of the rectangle R for $\tilde{C}$ (possibly entire R). We alter $\mathcal{R}$ by shortening all rectangles touching R inside this region by the same small amount $\varepsilon > 0$ and introducing a new rectangle R_c for c parallel to R at distance ε, touching all shortened rectangles and the rectangles R_A, R_B, R_a, R_b. Secondly, we let R be the rectangle for C. Then the resulting Plattenbau $\mathcal{R}$ represents G as its touching graph, and Items (I1) to (I4) hold for $\mathcal{R}$. □

Lemma 7 shows the sufficiency of Items (P1) to (P4). The necessity is given in Proposition 6. Together this proves Theorem 2.

4.1 Iterative Constructions for generic boxed Plattenbauten

We have given a characterization of graphs of generic boxed Plattenbauten as a generalization of plane quadrangulations. In this section, we show how these Plattenbauten can be constructed iteratively by inserting Plattenbauten into each other starting from the trivial one.

The following propositions give two different descriptions on the iterative structure of generic boxed Plattenbauten.

Proposition 8. *If $\mathcal{R}$ is a generic boxed Plattenbau with at least two rooms and Z is a room containing an outer corner, then Z has a side A_0, that is a rectangle of $\mathcal{R}$.*

Proof. Let o be an outer corner and Z be the room of $\mathcal{R}$ which contains o. Let $\bar{o}$ be the corner of Z which is opposite to o. Let A_0, A_1, A_2 be the three rectangles of $\mathcal{R}$ which form the sides of Z containing $\bar{o}$. Let A_0 be the one which has $\bar{o}$ as a corner, A_1 be the one which has $\bar{o}$ on a boundary edge, and A_2 be the one which has $\bar{o}$ as an interior point. This local structure at $\bar{o}$ shows that $A_0 \to A_1$, $A_0 \to A_2$, and $A_1 \to A_2$. The first two of these imply that A_0 is a rectangle of $\mathcal{R}$. □

Proposition 8 shows that a generic boxed Plattenbau $\mathcal{R}$ with outer corner o can be reduced to a trivial Plattenbau with only one room by repeating the following step: Identify the rectangle A_0, remove it and extend all the rectangles B with $B \to A_0$ such that the edge of B which made a contact with A_0 makes a contact with the outer rectangle which contains o and is parallel to A_0. This reduction also follows from the inductive proof of Theorem 2.

The next proposition gives a decomposition of generic boxed Plattenbauten by means of "stacking" Plattenbauten into Plattenbauten.

Proposition 9. *Let $\mathcal{R}$ be a generic boxed Plattenbau with inner rectangles in all three directions and r rooms. Then there are generic boxed Plattenbauten $\mathcal{R}_O$ and $\mathcal{R}_I$ with $r_O > 1$ and $r_I > 1$ rooms respectively and a room Z of $\mathcal{R}_O$, such that $\mathcal{R}$ can be obtained by inserting the inner rectangles of $\mathcal{R}_I$ in the room Z of $\mathcal{R}_O$, i.e., $r = r_o + r_I - 1$.*

Proof. Let x, y, z be the axes of the coordinate system. By translating and scaling the Plattenbau we may assume that the outer box of the Plattenbau is the cube spanned by $(0, 0, 0)$

and $(1,1,1)$. The outer rectangle in the $z=0$ plane is the *bottom rectangle* R_0 of $\mathcal{R}$. The *top rectangle* is the rectangle in a plane $z=1$, we denote it R_1. All the contacts of R_0 with inner rectangles are of type $A \to R_0$, i.e., $A \cap R_0$ is a segment on R_0.

If there is no inner rectangle A with $A \to R_0$, then there is a unique room Z with a side on R_0. Let B be the side of Z opposite of the R_0-side. Now let $R_I = \mathcal{R} - R_0$ and let R_O consist of the outer rectangles of R together with B, i.e., $r_O = 2$ and $r_I = r-1$.

From now on we assume that there is an inner rectangle A with $A \to R_0$, i.e., a segment in R_0. The union of all these segments yields a rectangular dissection D of the unit square $U \subseteq R_0$. With each inner segment s of D there is a rectangle R_s. Let z_s be the maximum z coordinate of a point in R_s, we refer to z_s as the height of R_s.

If s and s' are segments in R_0 and $R_s \to R_{s'}$, then $z_s \leq z_{s'}$ because the representation is proper. This shows that if we fix some h with $0 \leq h \leq 1$ and only look at segments $s \in D$ with $z_s > h$ we get a dissection D_h of U into rectangles. Let h^+ be the maximum value of z_s taken over inner segments $s \in D$.

If $h^+ = 1$ we use that the dissection D_1 is nontrivial and conclude that at least one of the rectangles of D_1 spans a box B between R_0 and R_1 which contains a rectangle A in a plane $z = h$ with $0 < h < a$. Let $\mathcal{R}_B$ be the set of all rectangles of $\mathcal{R}$ which are in B. Since $A \in \mathcal{R}_B$ this set is nonempty. Let $\mathcal{R}_I$ be $\mathcal{R}_B$ together with 6 outer rectangles covering the sides of B and let $R_O = \mathcal{R} - \mathcal{R}_B$. This is a decomposition as claimed.

If $h^+ < 1$ let D_+ be the dissection D_{h^+}. If D_+ contains a guillotine segment, i.e., a segment spanned between opposite sides of the outer square of D_+. Then we can permute the coordinates such that after the permutation we have $h^+ = 1$, i.e., we are in the previous case and have a nontrivial decomposition.

If $h^+ < 1$ and there is no guillotine segment, then the contact system of inner segments of D_+ is connected and for each of the outer segments there is an inner segment having a contact with it. Now consider two segments s and s' in D_+ such that $R_s \to R_{s'}$. Since $\mathcal{R}$ is generic there is some rectangle $T_{s'}$ containing the (open) top segment of $R_{s'}$ in the interior, i.e, $T_{s'}$ contains some ε stripe on both sides of the intersection of $R_{s'}$ with the plane $z = h^+$. Similarly there is a rectangle T_s containing the top segment of R_s. Hence, $T_{s'}$ and T_s intersect whence $T_{s'} = T_s$. Iterating this argument through all contacts of two segments of D^+ we find that there is a unique rectangle T such that $R_s \to T$ for all interior segments s of D_+. This shows that T spans the outer square of D_+. Now let $\mathcal{R}_B$ be the set of all rectangles of $\mathcal{R}$ which have z-coordinates between 0 and h^+, except T. This set is nonempty. Let $\mathcal{R}_I$ be $\mathcal{R}_B$ together with 6 outer rectangles covering the sides of B and let $R_O = \mathcal{R} - \mathcal{R}_B$. This is a decomposition as claimed. □

The count of combinatorially different generic boxed Plattenbauten with up to 5 rooms gives the numbers 1, 3, 15, 81, 495. The growth rate of the numbers p_n of generic boxed Plattenbauten with n rooms is only exponential, a rough estimate based on Proposition 9 yields $p_n \leq 48^n$. The sequence has no entry in the OEIS and deserves being studied in detail.

In a recent paper Fusy et al. [17] studied the enumeration of corner polyherdra, or equivalently of combinatorially different Plattenbau representations of 3-colorable triangulations. Using sophisticated bijections and analytic enumeration methods they establish a growth rate of $9/2$.

5 Conclusions

We have studied touching graphs of (generic) Plattenbauten as generalizations of planar bipartite graphs to space. Our first main result was that all 3-chromatic planar graphs belong to this class, in particular this shows that the recognition problem for the class is NP-complete. We also characterized the touching graphs of generic boxed Plattenbauten as a generalization of planar quadrangulations. However, a full characterization of touching graphs of (generic) Plattenbauten remains challenging.

With our results at hand it is natural to try and extend results from the planar setting to space. One example, is to attack a question asked by Jean Cardinal at the Order & Geometry Workshop at Gułtowy Palace in 2016: What is the 3-dimensional analogue of Baxter permutations? Since Baxter permutations are in bijection with boxed arrangements of axis-parallel segments in $\mathbb{R}^2$ [13], the question aims at finding permutation-like objects corresponding to generic boxed Plattenbauten. Our iterative constructions from Subsection 4.1 might help.

A natural continuation of this project is going to higher dimensions, i.e., consider touching graphs of cuboids of co-dimension one in $\mathbb{R}^d$. Already the class of 4-dimensional Plattenbau graphs contains all planar graphs, which follows from [31]. However, our constructions for planar 3-chromatic graphs could be generalized to higher dimensions, i.e., orthogonal subspaces in $\mathbb{R}^d$. A first interesting question here would be to characterize the skeleta of orthogonal subspaces in $\mathbb{R}^d$.

Finally, as suggested in the introduction, considering the intersection graph $I_{\mathcal{R}}$ instead of the touching graph of a Plattenbau, yields an interesting but very different graph class. The plane analogue of this is known as B_0-CPG graphs [5], yielding a first subclass. Another subclass are 4-connected planar graphs, since they have a rectangle contact representation in $\mathbb{R}^2$, see [23, 24, 28, 31, 33]. Also K_{12} is the intersection graph of the Plattenbau $\mathcal{R}$ consisting of the twelve axis-parallel unit squares in $\mathbb{R}^3$ that have a corner on the origin.

References

[1] Philip L. Bowers. Circle packing: a personal reminiscence. In Mircea Pitici, editor, *The Best Writing on Mathematics 2010*, pages 330–345. Princeton University Press, 2010.

[2] Adam L. Buchsbaum, Emden R. Gansner, Cecilia M. Procopiuc, and Suresh Venkatasubramanian. Rectangular layouts and contact graphs. *ACM Transactions on Algorithms*, 4(1), 2008. doi:10.1145/1328911.1328919.

[3] L. Sunil Chandran, Rogers Mathew, and Naveen Sivadasan. Boxicity of line graphs. *Discrete Mathematics*, 311(21):2359–2367, 2011. doi:10.1016/j.disc.2011.06.005.

[4] Hubert De Fraysseix and Patrice Ossona de Mendez. On topological aspects of orientations. *Discrete Mathematics*, 229(1):57–72, 2001. doi:10.1016/S0012-365X(00)00201-6.

[5] Zakir Deniz, Esther Galby, Andrea Munaro, and Bernard Ries. On contact graphs of paths on a grid. In *Proc. Graph Drawing and Network Visualization*, volume 11282 of *LNCS*, pages 317–330. Springer, 2018. doi:10.1007/978-3-030-04414-5_22.

[6] David Eppstein. Regular labelings and geometric structures. In *Proc. Canadian Conference on Computational Geometry*, pages 125–130, 2010. URL: `arxiv.org/abs/1007.0221`.

[7] David Eppstein and Elena Mumford. Steinitz theorems for simple orthogonal polyhedra. *Journal of Computational Geometry*, 5(1):179–244, 2014. doi:10.20382/jocg.v5i1a10.

[8] Stefan Felsner. Convex drawings of planar graphs and the order dimension of 3-polytopes. *Order*, 18:19–37, 2001. doi:10.1023/A:1010604726900.

[9] Stefan Felsner. *Geometric Graphs and Arrangements*. Vieweg Verlag, 2004. doi:10.1007/978-3-322-80303-0.

[10] Stefan Felsner. Lattice structures from planar graphs. *The Electronic Journal of Combinatorics*, 11(R15):24p., 2004. doi:10.37236/1768.

[11] Stefan Felsner. Rectangle and square representations of planar graphs. In J. Pach, editor, *Thirty Essays on Geometric Graph Theory*, pages 213–248. Springer, 2013. doi:10.1007/978-1-4614-0110-0_12.

[12] Stefan Felsner. The order dimension of planar maps revisited. *SIAM Journal on Discrete Mathematics*, 28:1093–1101, 2014. doi:10.1137/130945284.

[13] Stefan Felsner, Éric Fusy, Marc Noy, and David Orden. Bijections for Baxter families and related objects. *Journal of Combinatorial Theory, Series A*, 118(3):993–1020, 2011. doi:10.1016/j.jcta.2010.03.017.

[14] Stefan Felsner, Kolja Knauer, and Torsten Ueckerdt. Plattenbauten: Touching rectangles in space. In *Proc. Graph-Theoretic Concepts in Computer Science*, volume 12301 of *LNCS*, pages 161–173. Springer, 2020. doi:10.1007/978-3-030-60440-0_13.

[15] Stefan Felsner and Florian Zickfeld. Schnyder woods and orthogonal surfaces. *Discrete and Computational Geometry*, 40:103–126, 2008. doi:10.1007/s00454-007-9027-9.

[16] Éric Fusy. *Combinatoire des cartes planaires et applications algorithmiques*. PhD thesis, LIX Polytechnique, 2007. URL: `www.lix.polytechnique.fr/Labo/Eric.Fusy/Theses/these_eric_fusy.pdf`.

[17] Éric Fusy, Erkan Narmanli, and Gilles Schaeffer. Enumeration of corner polyhedra and 3-connected schnyder labelings. *Electron. Journal of Combinatorics*, 30(2), 2023. doi:10.37236/11174.

[18] Daniel Gonçalves. 3-colorable planar graphs have an intersection segment representation using 3 slopes. In *Proc. Graph-Theoretic Concepts in Computer Science*, volume 11789 of *LNCS*, pages 351–363. Springer, 2019. doi:10.1007/978-3-030-30786-8_27.

[19] Terja Hansen and Herbert Scarf. *The Computation of Economic Equilibria*, volume 24 of *Cowles Foundation Monograph*. Yale Univ. Press, 1973. URL: `lccn.loc.gov/73077165`.

[20] I.Ben-Arroyo Hartman, Ilan Newman, and Ran Ziv. On grid intersection graphs. *Discrete Mathematics*, 87(1):41–52, 1991. doi:10.1016/0012-365X(91)90069-E.

[21] Serkan Hoşten and Walter D. Morris. The order dimension of the complete graph. *Discrete Mathematics*, 201(1):133–139, 1999. doi:10.1016/S0012-365X(98)00315-X.

[22] Paul Koebe. Kontaktprobleme der konformen Abbildung. *Berichte über die Verhandlungen der Sächsischen Akademie der Wissenschaften zu Leipzig, Mathematisch-Physische Klasse*, 88:141–164, 1936.

[23] Krzysztof Koźmiński and Edwin Kinnen. Rectangular duals of planar graphs. *Networks*, 15(2):145–157, 1985. doi:10.1002/net.3230150202.

[24] Sany M Leinwand and Yen-Tai Lai. An algorithm for building rectangular floor-plans. In *Proc. 21st Design Automation Conference*, pages 663–664. IEEE, 1984. doi:10.1109/DAC.1984.1585874.

[25] Ezra Miller. Planar graphs as minimal resolutions of trivariate monomial ideals. *Documenta Mathematica*, 7:43–90, 2002. doi:10.4171/DM/117.

[26] Ezra Miller and Bernd Sturmfels. *Combinatorial Commutative Algebra*, volume 227 of *Graduate Texts in Mathematics*. Springer, 2004. doi:10.1007/b138602.

[27] János Pach, Hubert de Fraysseix, and Patrice Ossona de Mendez. Representation of planar graphs by segments. In K. Böröczky and G. Fejes Tóth, editors, *Intuitive Geometry*, Coll. Math. Soc. J. Bolyai 63, pages 109–117. North-Holland, 1994. URL: `infoscience.epfl.ch/record/129343/files/segments.pdf`.

[28] Pierre Rosenstiehl and Robert E Tarjan. Rectilinear planar layouts and bipolar orientations of planar graphs. *Discrete and Computational Geometry*, 1:343–353, 1986. doi:10.1007/BF02187706.

[29] Kenneth Stephenson. *Introduction to circle packing: The theory of discrete analytic functions*. Cambridge University Press, 2005. doi:10.1017/S0025557200180726.

[30] Roberto Tamassia and Ioannis G Tollis. A unified approach to visibility representations of planar graphs. *Discrete and Computational Geometry*, 1:321–341, 1986. doi:10.1007/BF02187705.

[31] Carsten Thomassen. Interval representations of planar graphs. *Journal of Combinatorial Theory, Series B*, 40(1):9–20, 1986. doi:10.1016/0095-8956(86)90061-4.

[32] Torsten Ueckerdt. *Geometric Representations of Graphs with Low Polygonal Complexity*. Doctoral thesis, Technische Universität Berlin, Fakultät II - Mathematik und Naturwissenschaften, Berlin, 2012. doi:10.14279/depositonce-3190.

[33] Peter Ungar. On diagrams representing maps. *Journal of the London Mathematical Society*, 28(3):336–342, 1953. doi:10.1112/jlms/s1-28.3.336.